Synthesis of tungsten complexes that contain hexaisopropylterphenyl-substituted triamidoamine ligands, and reactions relevant to the reduction of dinitrogen to ammonia

Dmitry V. Yandulov and Richard R. Schrock

Abstract: [HIPTN$_3$N]WCl (**W**Cl) can be synthesized readily by adding H$_3$[HIPTN$_3$N] to WCl$_4$(DME) followed by LiN(SiMe$_3$)$_2$ ([HIPTN$_3$N]$^{3-}$ = [(HIPTNCH$_2$CH$_2$)$_3$N]$^{3-}$ where HIPT = 3,5-(2,4,6-i-Pr$_3$C$_6$H$_2$)$_2$C$_6$H$_3$ = HexaIsoPropylTerphenyl). Reduction of **W**Cl with KC$_8$ in benzene under N$_2$ yields **W**N=NK. **W**N=NK is readily oxidized in THF by ZnCl$_2$ to yield zinc metal and **W**N$_2$. Reduction of **W**N$_2$ to [**W**N$_2$]$^-$ is reversible at –2.27 V vs. FeCp$_2$$^{+/0}$ in 0.1 mol/L [Bu$_4$N][BAr$'_4$]/PhF electrolyte (Ar$'$ = 3,5-(CF$_3$)$_2$C$_6$H$_3$), while oxidation of **W**N$_2$ to [**W**N$_2$]$^+$ is also reversible at –0.66 V. Protonation of **W**N=NK by [Et$_3$NH][OTf] in benzene yields **W**N=NH essentially quantitatively. Protonation of **W**N=NH at N$_\beta$ with [H(OEt)$_2$][BAr$'_4$] in ether affords [**W**=NNH$_2$][BAr$'_4$] quantitatively. Electrochemical reduction of [**W**=NNH$_2$][BAr$'_4$] in 0.1 mol/L [Bu$_4$N][BAr$'_4$]/PhF is irreversible at scan rates of up to 1 V/s. Addition of NaBAr$'_4$ and NH$_3$ to **W**Cl in PhF yields [**W**(NH$_3$)][BAr$'_4$]. Electrochemical reduction of [**W**(NH$_3$)][BAr$'_4$] in 0.1 mol/L [Bu$_4$N]-[BAr$'_4$]/PhF is irreversible at –2.06 V vs. FeCp$_2$$^{+/0}$ at a scan rate of 0.5 V/s. Treatment of [**W**(NH$_3$)][BAr$'_4$] with triethylamine and [FeCp$_2$][PF$_6$] in C$_6$D$_6$, followed by LiN(SiMe$_3$)$_2$, yielded **W**≡N. Treatment of [**W**(NH$_3$)][BAr$'_4$] with LiBHEt$_3$ (1 mol/L in THF) results in formation of **W**H, which is converted to **W**H$_3$ upon exposure to an atmosphere of H$_2$. Attempts to prepare **W**N=NH by treating **W**N$_2$ with [2,6-LutH][BAr$'_4$] and CoCp$_2$ yielded only [**W**=NNH$_2$][BAr$'_4$]. [**W**=NNH$_2$][BAr$'_4$] is reduced to **W**=NNH$_2$ by CoCp$^*_2$, but this species disproportionates to yield **W**N=NH, **W**≡N, and ammonia. Reduction of [**W**(NH$_3$)][BAr$'_4$] with CoCp$^*_2$ does not yield any observable **W**(NH$_3$). Attempted catalytic reduction of dinitrogen using **W**N$_2$ as the catalyst under conditions identical or similar to those employed for catalytic reduction of dinitrogen by **Mo**N$_2$ and related Mo complexes failed. Single crystal X-ray studies were carried out on **W**-N=NK, **W**N$_2$, **W**-N=NH, [**W**=NNH$_2$][BAr$'_4$], and [**W**(NH$_3$)][BAr$'_4$].

Key words: dinitrogen, reduction, tungsten, ammonia.

Résumé : Le complexe [HIPTN$_3$N]WCl (**W**Cl) peut facilement être synthétisé par l'addition de H$_3$[HIPTN$_3$N] à du WCl$_4$(DME), suivie d'une additon de LiN(SiMe$_3$)$_2$ ([HIPTN$_3$N]$^{3-}$ = [(HIPTNCH$_2$CH$_2$)$_3$N]$^{3-}$ dans lequel HIPT = 3,5-(2,4,6-i-Pr$_3$C$_6$H$_2$)$_2$C$_6$H$_3$ = HexaIsoPropylTerphényle). La réduction de **W**Cl par du KC$_8$, dans du benzène, sous atmosphère d'azote, conduit à la formation de **W**N=NK. Sous l'action du ZnCl$_2$ dans du THF, le **W**N=NK s'oxyde facilement pour conduire à la formation de zinc métallique et de **W**N$_2$. Dans un électrolyte à 0,1 mol/L de [Bu$_4$N][BAr$'_4$]/PhF (Ar$'$ = 3,5-(CF$_3$)$_2$C$_6$H$_3$), la réduction du **W**N$_2$ en [**W**N$_2$]$^-$ est réversible à –2,27 V vs. FeCp$_2$$^{+/0}$ alors que l'oxydation du [**W**N$_2$] en [**W**N$_2$]$^+$ est aussi réversible à –0,66 V. La protonation du **W**N=NK par le [Et$_3$NH][OTf], dans le benzène, conduit à la formation de **W**N=NH, avec un rendement pratiquement quantitatif. La protonation du **W**N=NH au niveau du N$_\beta$ avec du [H(OEt)$_2$][BAr$'_4$], dans l'éther, conduit à la formation de [**W**=NNH$_2$][BAr$'_4$] avec un rendement quantitatif. La réduction électrochimique du [**W**=NNH$_2$][BAr$'_4$] dans du [Bu$_4$N][BAr$'_4$]/PhF à 0,1 mol/L est irréversible à des vitesses de balayage allant jusqu'à 1 V/s. L'addition de NaBAr$'_4$ et de NH$_3$ au **W**Cl dans du PhF conduit à la formation de [**W**(NH$_3$)][BAr$'_4$]. La réduction électrochimique du [**W**(NH$_3$)][BAr$'_4$] dans du [Bu$_4$N][BAr$'_4$]/PhF à 0,1 mol/L est irréversible à –2,06 V vs. FeCp$_2$$^{+/0}$, à une vitesse de balayage de 0,5 V/s. Le traitement du [**W**(NH$_3$)][BAr$'_4$] par de la triéthylamine et du [FeCp$_2$][PF$_6$] dans du C$_6$D$_6$, suivi de LiN(SiMe$_3$)$_2$ conduit à la formation de **W**≡N. Le traitement de [**W**(NH$_3$)][BAr$'_4$] par du LiBHEt$_3$ (1 mol/L dans du THF) conduit à la formation de **W**H qui peut être transformé en **W**H$_3$ par exposition à un atmosphère de H$_2$. Des essais en vue de préparer le **W**N=NH par traitement du **W**N$_2$ avec du [2,6-LutH][BAr$'_4$] et du CoCp$_2$ ne fournissent que du [**W**=NNH$_2$][BAr$'_4$]. Sous l'influence du CoCp$^*_2$, le [**W**=NNH$_2$]-[BAr$'_4$] est réduit en **W**=NNH$_2$, mais cette espèce subit une réaction de dismutation conduisant à la formation de **W**N=NH, de **W**≡N et d'ammoniac. La réduction du [**W**(NH$_3$)][BAr$'_4$] par le CoCp$^*_2$ ne fournit aucune trace de **W**(NH$_3$). Des essais en vue d'effectuer la réduction du diazote en utilisant du **W**N$_2$ comme catalyseur, dans des

Received 11 August 2004. Published on the NRC Research Press Web site at http://canjchem.nrc.ca on 30 March 2005.

D.V. Yandulov[1] and R.R. Schrock.[2] Department of Chemistry, Massachusetts Institute of Technology, Cambridge, MA 02139, USA.

[1] Present address: Department of Chemistry, Stanford University, Stanford, CA 94305-5080, USA.
[2] Corresponding author (e-mail: rrs@mit.edu).

doi: 10.1139/V05-013

conditions identiques ou semblables à celles utilisées pour la réduction catalytique du diazote par le **Mo**N_2 et les complexes apparentés du molybdène n'ont pas donné les résultats escomptés. Des études de diffraction des rayons X sur un cristal unique ont été effectuées sur le **W**-N=NK, le **W**N_2, le **W**-N=NH, le [**W**=NNH_2][BAr'_4] et le [**W**(NH_3)][BAr'_4].

Mots clés : diazote, réduction, tungstène, ammoniac.

[Traduit par la Rédaction]

Introduction

Discovery of the first dinitrogen complex of a transition metal, $[Ru(NH_3)_5(N_2)]^{2+}$, in 1965 (1) provided support for the proposal that dinitrogen might be reduced to ammonia at a molybdenum center in nitrogenase (only the FeMo nitrogenase was known at the time (2–4)). As more and more types of transition-metal-catalyzed reactions were discovered in the following decades, scientists became optimistic that catalysts would be discovered for the reduction of dinitrogen to ammonia, or for the combination of dinitrogen with elements other than hydrogen (5–16). Unfortunately, although hundreds of man years have been directed toward this goal in the last 40 years, and although hundreds of dinitrogen complexes of all transition metals in groups 4 through 10 (if we include those detected at low temperature in matrices) are now known, progress has been relatively slow.

Chatt, a pioneer, along with Hidai, in dinitrogen chemistry involving W(0) and Mo(0) phosphine complexes (5–7, 12, 14) believed that dinitrogen could be reduced to ammonia at a single metal center through end-on binding of dinitrogen, and was the first to show that up to 2 equiv. of ammonia per metal could be formed from M(0) dinitrogen complexes (M = Mo or W) upon addition of protons, the six electrons being provided by the metal (5). If dinitrogen could be reduced to ammonia catalytically through the addition of six external protons and six external electrons, and if a distinct intermediate were formed upon addition of each proton and electron, then 12 intermediates could be imagined, or a total of 14 if one includes a dinitrogen complex and a complex that contains no nitrogen or nitrogen-derived ligand. Although examples of almost all of the proposed intermediates for reduction of dinitrogen at a single Mo or W center in a "Chatt cycle" have been isolated, the ligand environment (L_x) of the metal has varied from compound to compound, and no catalytic reaction to give ammonia was ever achieved (see, however, the synthesis of silylamines catalytically (17)). Significant progress has been made toward utilizing atmospheric dinitrogen to make organic molecules (6, 7, 18–26). One catalytic reduction is known in which dinitrogen is reduced to a mixture of hydrazine (largely) and ammonia (9, 27, 28). This system requires molybdenum, is catalytic with respect to molybdenum, produces >90% hydrazine, and takes place in methanol in the presence of $Mg(OH)_2$ and a strong reducing agent (e.g., Na amalgam). Unfortunately, few details concerning the mechanism of this intriguing reaction have been established. In this context, it should be noted that ammonia can be formed from hydrazine via disproportionation (to dinitrogen and ammonia) in the presence of transition metals. In fact, $[Ru(NH_3)_5(N_2)]^{2+}$ was first prepared by treating Ru salts with hydrazine (1).

Fig. 1. A drawing of $[HIPTN_3N]Mo(N_2)$ = **Mo**N_2.

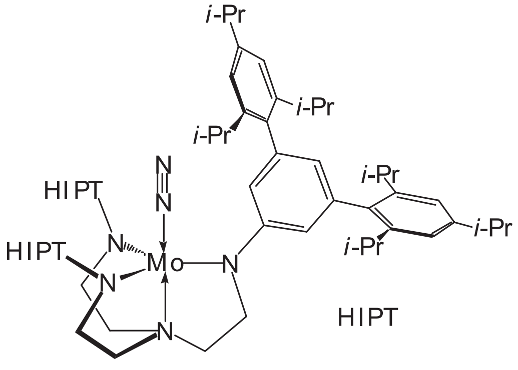

1

We have been interested in dinitrogen chemistry of early metals in relatively high oxidation states for more than two decades (29). Approximately 4 years ago, we began to explore the chemistry of Mo complexes that contain a triamidoamine ($[(ArNCH_2CH_2)_3N]^{3-}$ = $[ArN_3N]^{3-}$, Ar = aryl) ligand (30, 31). To prevent formation of what we believe to be relatively stable and unreactive bimetallic $[ArN_3N]$Mo-N=N-Mo$[ArN_3N]$ complexes, maximize steric protection of a metal coordination site in a monometallic species, and provide increased solubility in nonpolar solvents, we synthesized species that contain a $[HIPTN_3N]^{3-}$ ligand, where HIPT = $3,5\text{-}(2,4,6\text{-}i\text{-}Pr_3C_6H_2)_2C_6H_3$ (HexaIsoPropylTerphenyl, see Fig. 1) (32, 33). Starting with **Mo**Cl (**Mo** = $[HIPTN_3N]$Mo), we showed that we could isolate and characterize many intermediates in a hypothetical Chatt-like reduction of dinitrogen, all of which contain the same $[HIPTN_3N]^{3-}$ supporting ligand (Fig. 2). These intermediates include paramagnetic **Mo**(N_2) (**1**), diamagnetic [**Mo**(N_2)]$^-$ (**2**), diamagnetic **Mo**-N=N-H (**3**), diamagnetic {**Mo**=N-NH_2}{BAr'_4} (**4**; Ar′ = $3,5\text{-}(CF_3)_2C_6H_3$), diamagnetic Mo≡N (**7**), diamagnetic {**Mo**=NH}{BAr'_4} (**8**), paramagnetic {**Mo**(NH_3)}{BAr'_4} (**12**), and paramagnetic **Mo**(NH_3) (**13**). Extensive ^{15}N labeling studies, NMR studies, and X-ray studies (of **1**, **2** (as two different Mg derivatives), **7**, and **12** (33), and **3**, **4**, **8**, and **13** (34)) all reveal a trigonal pocket in which N_2 or its reduced products are protected to a dramatic degree by three $3,5\text{-}(2,4,6\text{-}i\text{-}Pr_3C_6H_2)_2C_6H_3$ (HIPT) rings clustered around it. Compounds **5**, **6**, **10**, and **14** (Fig. 2) have not yet been observed. The oxidation state of the metal varies between Mo(III) and Mo(VI) in the species as they are drawn in Fig. 2. No other unambiguous example of one of these complexes (**3**) is known, presumably either because in other systems bimolecular processes that involve H radical or proton transfer result in facile decomposition, or the synthetic methods are incompatible with the ligands that are present. Steric protection of the nitrogen entities within the pocket provided by the bulky HIPT groups are believed to be an important reason why several of the most unusual species can be prepared.

Fig. 2. Proposed intermediates in the reduction of dinitrogen at a [HIPTN$_3$N]Mo (**Mo**) center through the step-wise addition of protons and electrons.

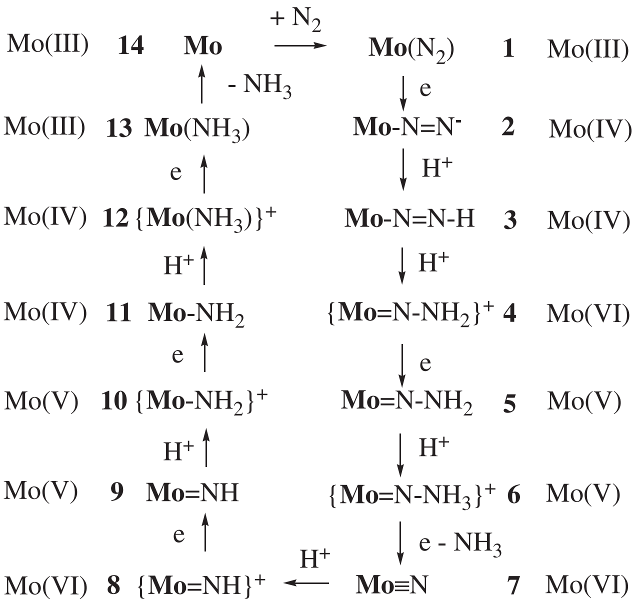

We then showed that it is possible in fact to reduce dinitrogen catalytically in heptane using {2,6-lutidinium}{BAr$'_4$} as the proton source and decamethylchromocene as the electron source (35). The results of 16 runs using four different Mo derivatives (**1**, **3**, **7**, or **12**) revealed that ~8 equiv. of ammonia are formed with an efficiency of 63%–66% based on reducing equivalents available. A run employing **Mo**(^{15}N^{15}NH) under $^{15}N_2$ yielded entirely ^{15}N-labeled ammonia. We assume at this stage that any equivalents of reducing agent that are not consumed in making ammonia are consumed to form hydrogen, and we now know that no hydrazine is formed.[3] The fact that compounds that contain hexamethylterphenyl or hexa-*tert*-butylterphenyl variations of the [HIPTN$_3$N]$^{3-}$ ligand are relatively inefficient catalysts for catalytic reduction of dinitrogen to ammonia (37) suggests that the catalytic reaction is extremely finely balanced and that perhaps most or all of the intermediates shown in Fig. 2 are actually involved. All are likely to be equilibria with exception of the actual N—N bond cleavage reaction (**Mo**=N-NH$_3^+$ + e → **Mo**≡N + NH$_3$).

It has been known for some time that certain bacteria grown in the presence of tungsten will produce a "FeW nitrogenase", but that enzyme will not reduce dinitrogen to ammonia (2, 3, 38). Therefore, we became interested in preparing some tungsten analogs of the [HIPTN$_3$N]Mo species shown in Fig. 2, exploring conversion of one to another, and testing at least one of them for catalytic dinitrogen reduction activity. We report this work here.

Results

Synthesis of WCl and diazenido species

The starting material for this chemistry ([HIPTN$_3$N]WCl (**W**Cl)) can be readily synthesized by a two-step method analogous to that used to prepare [HIPTN$_3$N]MoCl (33) as shown in eq. [1]. The ^{1}H NMR spectrum of high-spin **W**Cl (d^2) contains sharper resonances than does the spectrum of **Mo**Cl; this difference, and the pattern of relative shifts of the corresponding resonances between Mo and W complexes is very similar to that observed previously for a series of related [ArN$_3$N]MCl (M = Mo, W) (30, 39, 40) and [Me$_3$SiN$_3$N]MCl (41–43) complexes. Like **Mo**Cl, **W**Cl is exceedingly air- and moisture sensitive, so the utmost care is required to ensure that solvents are pure, dry, and free of oxygen.

Reduction of **Mo**Cl with magnesium in THF under an atmosphere of dinitrogen led to salts that contain the [**Mo**(N$_2$)]$^-$ anion (33). However, attempts to prepare [**W**(N$_2$)]$^-$ salts in this manner were not successful; **W**Cl was slowly converted into a complex mixture of unidentified products. Reduction of **W**Cl is markedly accelerated when potassium graphite (KC$_8$) is employed as the reductant in THF or DME, but a complex mixture of products is still formed. However, when **W**Cl is treated with KC$_8$ in benzene under dinitrogen, clean and nearly quantitative conversion of **W**Cl to diamagnetic **W**-N=NK takes place over a period of 1 to 2 days at room temperature (eq. [2]). No intermediates could be detected by ^{1}H NMR when this reaction was performed in C$_6$D$_6$. Deep red **W**-N=NK was isolated in good yield and was fully characterized. Since **W**-N=NK can be dissolved in THF without decomposition (vide infra), failure of the reductions in THF and DME must be attributed to a some side reaction or reactions prior to binding of dinitrogen to the metal, presumably at the W(III) stage. **W**N=NK is readily soluble in aliphatic

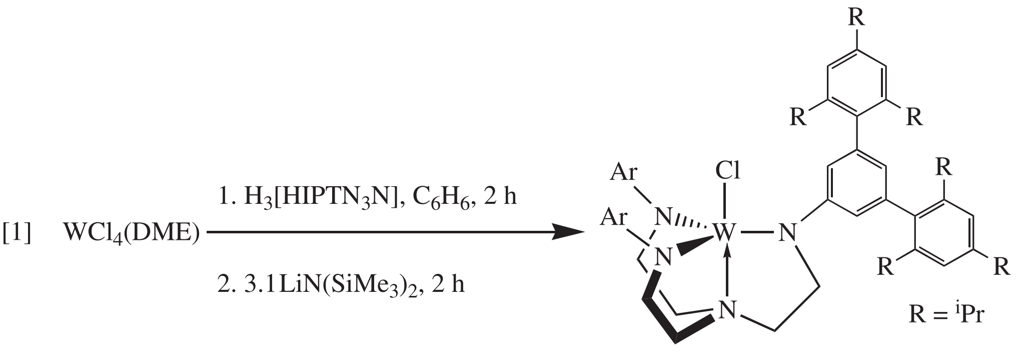

WCl

---

[3] W. Weare. Unpublished results.

Fig. 3. Thermal ellipsoid drawing of **W**N=NK (50% probability level, hydrogen atoms omitted).

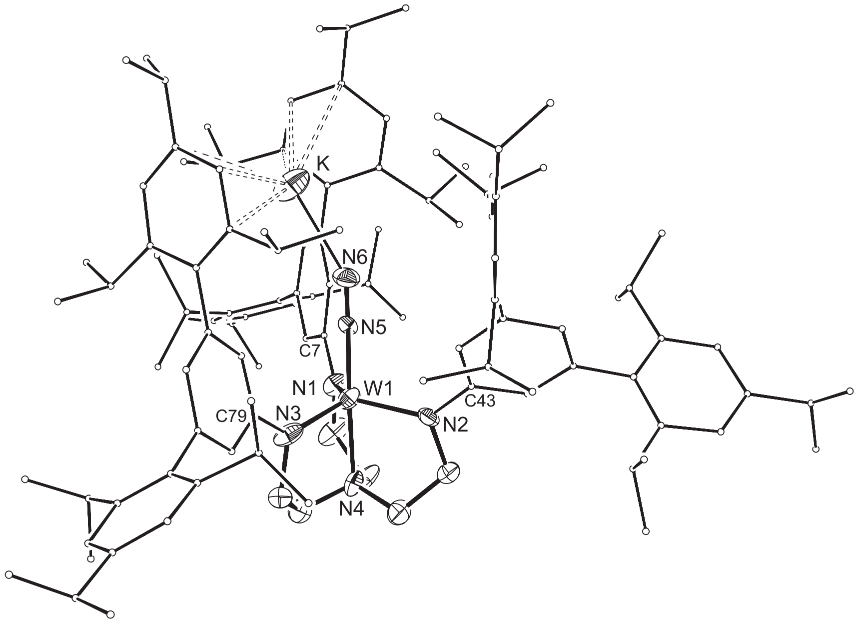

[2] 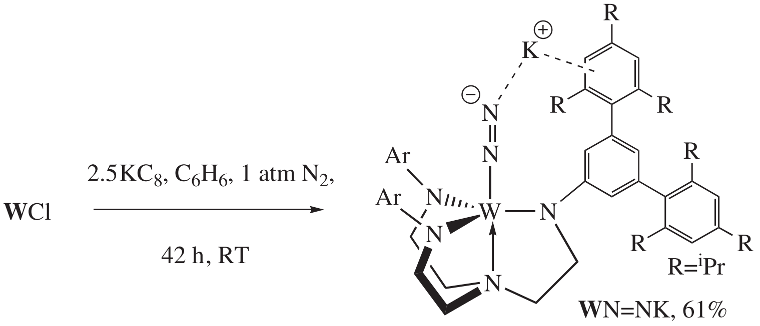

solvents and can be recrystallized without change from pentane.

The structure of **W**-N=NK, as determined through a single crystal X-ray study, is shown in Fig. 3 (see also Table 1 for crystal data and Table 2 for selected M—N and N—N bond distances and angles in W and Mo analogs, along with selected IR and NMR data. A full set of X-ray data is available as supporting information.[4] The potassium ion is 2.536(7) Å from N6, the β nitrogen in the unsubstituted diazenido ligand, and is supported through six interactions with aryl carbon atoms in two Trip (2,4,6-i-Pr$_3$C$_6$H$_2$) aromatic rings of two HIPT substituents. The potassium ion resides 3.229 and 3.301 Å from the ring centroids, and all K···H contacts are >2.92 Å. Interaction between the potassium and the aromatic rings is not symmetric, with K···C distances spanning a range of 0.52 Å for each ring. The presence of the potassium ion has no noticeable effect on the C—C bond distances in the two aryl rings with which it interacts. Understandably, the orientations of the three HIPT groups are significantly different, with one HIPT group in contact with K being rotated by only 10° out of the plane of the amide nitrogen (N1), while the other two HIPT groups are rotated by an average of 28.3° outside of the plane of the amide nitrogen to which they are attached. "Encapsulation" of the K ion between two aryl rings accounts for the high solubility of **W**-N=NK in aliphatic solvents (binding of sodium or potassium ions to aryl rings in high oxidation state amido complexes has considerable precedent in the literature (44–47)). The N—N (1.220(8) Å) and W—N (1.849(7) Å) bond distances are consistent with a considerably greater degree of reduction of the N$_2$ unit in **W**-N=NK relative to that in **Mo**-N=NMgBr(THF)$_3$ (1.156(8) and 1.863(7) Å, respectively) (33). Greater backbonding from the tungsten center in **W**-N=NK (vs. the molybdenum center in **Mo**-N=NMgCl(THF)$_3$ (33)) is also evident from the relative values for ν_{NN} in the two species (1745 cm^{-1} (W) and 1812 cm^{-1} (Mo), respectively, in benzene). The W-N$_\alpha$-N$_\beta$ angle is essentially linear (177.3(6)°), as expected.

---

[4] Supplementary data may be purchased from the Directory of Unpublished Data, Document Delivery, CISTI, National Research Council Canada, Ottawa, ON K1A 0S2, Canada (http://cisti-icist.nrc-cnrc.gc.ca/irm/unpub_e.shtml for information on ordering electronically). CCDC 261864–261868 contain the crystallographic data for this manuscript. These data can be obtained, free of charge, via www.ccdc.cam.ac.uk/conts/retrieving.html (or from the Cambridge Crystallographic Data Centre, 12 Union Road, Cambridge CB2 1EZ, U.K.; fax +44 1223 336033; or deposit@ccdc.cam.ac.uk).

Table 1. Crystal data and structure refinement for [HIPTN$_3$N]W-N=NK, [HIPTN$_3$N]WN$_2$, [HIPTN$_3$N]W-N=NH, {[HIPTN$_3$N]W=N-NH$_2$}[BAr$'_4$], and {[HIPTN$_3$N]W(NH$_3$)}[BAr$'_4$].[a]

	W-N=NK	**W**N$_2$	**W**-N=NH	{**W**-N=NH$_2$}[BAr$'_4$]	{**W**(NH$_3$)}[BAr$'_4$]
Empirical formula	$C_{114}H_{159}KN_6W$	$C_{114}H_{159}N_6W$	$C_{114}H_{160}N_6W$	$C_{146}H_{173}BF_{24}N_6W$	$C_{146}H_{174}BF_{24}N_5W$
Formula weight	1 836.42	1 797.32	1 798.33	2 662.56	2649.56
Crystal system	Monoclinic	Monoclinic	Triclinic	Triclinic	Triclinic
Space group	$P2(1)/n$	Cc	$P\bar{1}$	$P\bar{1}$	$P\bar{1}$
a (Å)	18.297(4)	16.0231(9)	18.2377(14)	15.7795(10)	15.8411(9)
b (Å)	40.166(9)	40.125(2)	20.1004(15)	20.6647(14)	20.5894(11)
c (Å)	19.528(4)	17.9933(10)	37.763(3)	26.2549(17)	26.3012(14)
α (°)	90	90	86.923(2)	85.2740(10)	84.9740(10)
β (°)	117.600(5)	93.8110(10)	85.346(2)	83.6730(10)	83.8560(10)
γ (°)	90	90	75.098(2)	81.9220(10)	81.8820(10)
Volume (Å^3)	12 718(5)	11 542.7(11)	13 326.0(17)	8405.1(10)	8420.7(8)
Z	4	4	4	2	2
Density (calcd., Mg/m^3)	0.959	1.034	0.896	1.052	1.045
Absorption coeff. (mm^{-1})	0.981	1.044	0.904	0.755	0.754
F(000)	3912	3836	3840	2772	2760
Crystal size (mm^3)	0.20 × 0.18 × 0.07	0.27 × 0.15 × 0.14	0.20 × 0.10 × 0.03	0.21 × 0.14 × 0.12	0.18 × 0.16 × 0.13
θ range (°)	1.01–25.00	1.37–27.00	1.05–25.00	0.78–27.00	0.78–27.00
Index ranges	$-14 \le h \le 21$	$-20 \le h \le 20$	$-21 \le h \le 18$	$-18 \le h \le 20$	$-20 \le h \le 20$
	$-47 \le k \le 47$	$-50 \le k \le 51$	$-23 \le k \le 15$	$-26 \le k \le 25$	$-15 \le k \le 26$
	$-21 \le l \le 23$	$-10 \le l \le 22$	$-44 \le l \le 44$	$-33 \le l \le 33$	$-33 \le l \le 33$
Reflections collected	62 953	35 587	69 284	57 366	57 597
Indep. reflections (R(int))	22 389 (0.1916)	16 642 (0.0509)	46 258 (0.1000)	36 498 (0.0387)	36 583 (0.0817)
Compl. to θ max (%)	99.9	99.9	98.6	99.4	99.5
Absorption correction	None	None	Empirical[b]	Empirical[b]	None
Data/restraints/param.	22 389/0/1 135	16 642/2/1 126	46 258/21/2 251	36 498/0/1 639	36 583/0/1 631
Goodness-of-fit on F^2	0.938	0.965	0.928	0.961	0.776
Final R indices ($I > 2\sigma(I)$)	$R1 = 0.0733$	$R1 = 0.0434$	$R1 = 0.1026$	$R1 = 0.0611$	$R1 = 0.0612$
	$wR2 = 0.1517$	$wR2 = 0.0984$	$wR2 = 0.2264$	$wR2 = 0.1489$	$wR2 = 0.1147$
R indices (all data)	$R1 = 0.1362$	$R1 = 0.0504$	$R1 = 0.2094$	$R1 = 0.0805$	$R1 = 0.1048$
	$wR2 = 0.1732$	$wR2 = 0.1004$	$wR2 = 0.2632$	$wR2 = 0.1577$	$wR2 = 0.1235$
Peak and hole (e Å^{-3})	2.872 and –1.777	1.765 and –1.530	1.295 and –1.619	2.172 and –1.566	1.244 and –1.090

[a] In all cases the temperature = 193(2) K, the wavelength = 0.710 73 Å, and the refinement method full-matrix least-squares on F^2.
[b] Empirical absorption correction was applied using the SADABS v2.10 program (36).

Table 2. A comparison of structural and spectroscopic properties of selected [HIPTN$_3$N]W and [HIPTN$_3$N]Mo complexes.[a]

Compound property	**Mo**N$_2$	**W**N$_2$	**W**N=NK	**Mo**N=NH	**W**N=NH	**Mo**=NNH$_2$$^{+b}$	**W**=NNH$_2$$^{+b}$
M-N$_\alpha$ (Å)	1.963(5)	1.945(6)	1.849(7)	1.810(7)	1.732(9)	1.737(3)	1.745(3)
N$_\alpha$-N$_\beta$ (Å)	1.061(7)	1.132(8)	1.220(8)	1.25(1)	1.29(1)	1.310(5)	1.315(5)
$\nu(^{14}N_\alpha{}^{14}N_\beta)$ (cm^{-1})	1990	1888	1745	1587	1542	—	—
$\nu(^{15}N_\alpha{}^{15}N_\beta)$ (cm^{-1})	1924	1826	1688	1523	1499	—	—
$\delta(^{15}N_\alpha{}^{15}N_\beta)$ (ppm)	—	—	357, 350	409, 233	394, 229	358, 140	344, 131
$^1J(^{15}N_\beta{}^{15}N_\alpha$, H) (Hz)	—	—	11.2	15.9, 53.6	15.4, 53.1	11.2, 90.5	10.1, 83.6

[a] IR and ^{15}N NMR data in C_6D_6 at 22 °C, unless stated otherwise. The Mo compounds can be found in refs. 33 and 34.
[b] Anion = BAr$'^{-}_4$.

Doubly labeled **W**-^{15}N=^{15}NK reveals sharp doublet resonances for $^{15}N_\alpha$ (at 357 ppm) and $^{15}N_\beta$ (at 350 ppm) in the ^{15}N NMR spectrum in C_6D_6 at room temperature. The $^{15}N_\alpha$ and $^{15}N_\beta$ resonances in **W**-^{15}N=^{15}NK are relatively close together, yet fall well within the range typical for compounds of this general type (48, 49). The ^{1}H NMR spectrum of **W**-N=NK in C_6D_6 at room temperature features slightly broadened resonances, yet is otherwise consistent with a C_{3v}-symmetric structure. Apparently the interactions between the potassium ion and the aryl rings are weak enough so that intramolecular ligand fluxionality in **W**-N=NK, including rotation of the HIPT rings around the N—C$_{ipso}$ bonds, is not hindered significantly at room temperature.

Treatment of a C_6D_6 solution of **W**-N=NK with Bu$_4$NCl results in a rapid color change from maroon-red to dark green. Both IR and ^{1}H NMR spectra of the green solution show complete conversion of **W**-N=NK to a single diamagnetic product with a ν_{NN} frequency shifted to higher energy

Fig. 4. Thermal ellipsoid drawing of **W**N_2 (50% probability level, hydrogen atoms omitted).

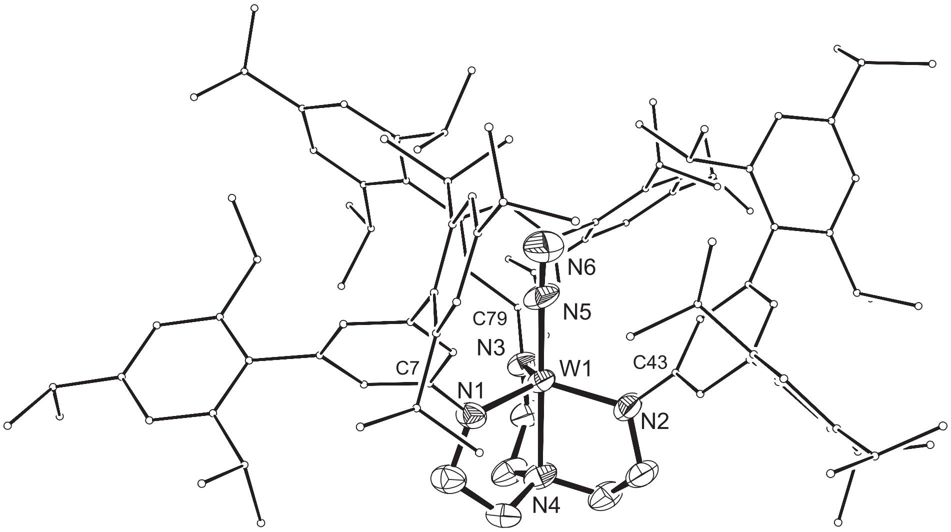

by 56 cm^{-1} from what it is in **W**-N=NK. These observations are analogous to those made for related **Mo** diazenides (33) and indicate formation of a species in which there is essentially no interaction between the cation and the β nitrogen, i.e., formation of [**W**-N=N]$^-$. However, all attempts to crystallize [**W**-N=N][Bu_4N] (e.g., by precipitation with pentane) have failed. This compound appears to decompose to yield two major pentane-soluble diamagnetic tungsten complexes and Bu_3N. We speculate that part of the decomposition consists of a reaction between [**W**N_2]$^-$ and Bu_4N^+ to yield **W**-N=NBu and Bu_3N. In contrast, [**Mo**-N=N][Bu_4N] can be isolated and is stable at room temperature (33). A greater nucleophilicity of [**W**N_2]$^-$ compared to [**Mo**N_2]$^-$ at N_β would be consistent with the observed greater degree of backbonding from tungsten to the N_2 unit and would not be surprising.

Synthesis of a terminal dinitrogen complex of W(III)

Like various {**Mo**-N=N}$^-$ salts (33), **W**N=NK is readily oxidized in THF by $ZnCl_2$ to yield zinc metal and the neutral dinitrogen complex, **W**N_2, essentially quantitatively. The **W**N_2 complex was isolated as an orange solid in 53% yield starting from **W**Cl and has been fully characterized. The ^1H NMR spectrum of **W**N_2 in C_6D_6 resembles that of the low-spin d^3 **Mo**N_2 analog (33), although the ligand backbone resonances of the **W** complex are broader and shifted with respect to those for **Mo**N_2 (at 35, –11, and –23 ppm for **W**N_2 and at 23 (NCH_2), –5 (4,6-H), and –34 (NCH_2) ppm in **Mo**N_2). **W**N_2 is the only known terminal dinitrogen complex of tungsten in which a triamido/amine ligand is present and the only one of W(III) to our knowledge.

A single crystal X-ray study of **W**N_2 (Fig. 4) shows it to have a structure analogous to that of **Mo**N_2 (33) with an N—N bond distance of 1.132(8) Å (cf. 1.098 Å in free N_2 and 1.061(7) Å in **Mo**N_2). The observed “shorter” N—N bond length in **Mo**N_2 than in free dinitrogen is believed to be a consequence of a slight “libration” of the bound dinitrogen about the center of the N—N bond, which would make the N—N bond appear slightly shorter than it actually is (34). The actual N—N bond distance in **W**N_2 therefore actually also could be somewhat longer than what is observed, although one might expect the degree of this type of libration of a bound dinitrogen to decrease as backbonding to dinitrogen increases. There is clearly a greater degree of backbonding to N_2 in **W**N_2 than in **Mo**N_2 also according to ν(N-N) frequencies, i.e., the value for ν(N-N) is nearly 100 cm^{-1} lower in **W**N_2 (1888 cm^{-1}) than in **Mo**N_2 (1990 cm^{-1}). All other structural details are normal for [$HIPTN_3N$]$^{3-}$ complexes (see supporting information).[4]

Fig. 5. Electrochemical behavior of **M**N_2 (**M** = **Mo** or **W**) in 0.1 mol/L [Bu_4N][BAr'_4]/PhF, recorded at a glassy carbon electrode (3 mm diam.) at a scan rate of 500 mV/s. The potential scale is referenced to $FeCp_2^{+/0}$.

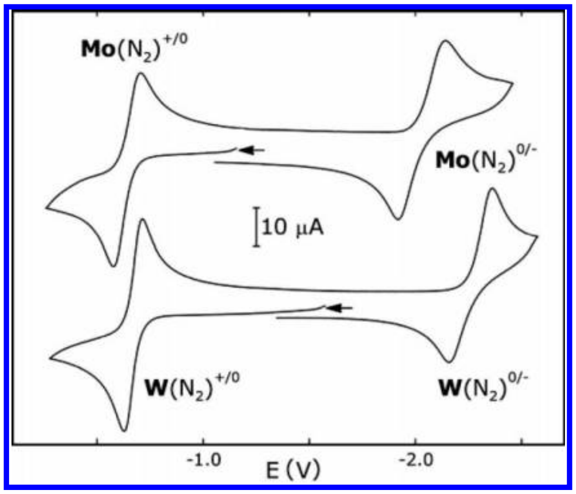

Electrochemical reduction of **W**N_2 to [**W**N_2]$^-$ is reversible and takes place at –2.27 V vs. $FeCp_2^{+/0}$ in 0.1 mol/L [Bu_4N][BAr'_4]/PhF electrolyte (Fig. 5) (the advantages of [Bu_4N]$^+$ salts of relatively unreactive and weakly coordinating anions as electrolytes in polar, but relatively unreactive solvents such as fluorobenzene, were demonstrated more than 10 years ago (50), and have been explored more systematically by Geiger and co-workers in the last several years (51–55)). The **W**$N_2^{0/-}$ potential is 260 mV more negative than the corresponding $E^{\circ\prime}$(**Mo**$N_2^{0/-}$) value (34), consistent with tungsten being more difficult to reduce than molybdenum, as expected. The tungsten dinitrogen complex also undergoes a reversible electrochemical oxidation, but at the *same* potential as the molybdenum dinitrogen complex (–0.66 V, Fig. 5). The similarity in the $\mathbf{M}N_2{}^{+/0}$ potentials for Mo and W can be ascribed to an effective "leveling" of the HOMO energies in the two $\mathbf{M}N_2$ complexes as a consequence of increased π donation from the metal to N_2 in $\mathbf{W}N_2$ ($\Delta\nu$(N-N) = 102 cm^{-1}, vide supra). However, the HOMO energies in $[\mathbf{Mo}N_2]^-$ and $[\mathbf{W}N_2]^-$ are not approximately the same, and $[\mathbf{W}N_2]^-$ therefore remains a stronger one-electron reductant than $[\mathbf{Mo}N_2]^-$ by 260 mV under the conditions described.

Synthesis of WN=NH and $[W{=}NNH_2][BAr'_4]$

Protonation of **W**N=NK by $[Et_3NH][OTf]$ in benzene is virtually instantaneous and yields **W**N=NH essentially quantitatively (eq. [3]). Diamagnetic **W**N=NH was isolated in 55% yield starting from **W**Cl and has been fully characterized. The N=N*H* resonance appears at 8.43 ppm in the ^1H NMR spectrum in C_6D_6, flanked by ^{183}W satellites with $^3J(^{183}W\text{-}H)$ = 17.4 Hz. The IR spectrum in C_6D_6 exhibits a ν(N-N) absorption at 1542 cm^{-1}, a frequency 45 cm^{-1} lower than the corresponding value in **Mo**N=NH (34). The ^1H NMR spectrum of doubly labeled $\mathbf{W}\text{-}^{15}N{=}^{15}NH$ features a doublet of doublets for the $^{15}N{=}^{15}NH$ resonance ($^1J(^{15}N_\beta\text{-}H)$ = 53.1 Hz, $^2J(^{15}N_\alpha\text{-}H)$ = 6.7 Hz) and two doublets of doublets at 394 ($^{15}N_\alpha$) and 229 ($^{15}N_\beta$) ppm ($^1J(^{15}N\text{-}^{15}N)$ = 15.4 Hz) in the ^{15}N NMR spectrum. These NMR data are similar to those observed for **Mo**N=NH (Table 2). Unlike **Mo**N=NH, however, **W**N=NH is quite stable thermally, suffering only minor decomposition after a solution in C_6D_6 had been heated to 65 °C for 11 days. In contrast, **Mo**N=NH decays in C_6D_6 with a half-life of ~7 h at 61 °C, forming predominantly **Mo**H, when prepared via a method analogous to that shown in eq. [3]. This decomposition was shown to be promoted by traces of acid (33) that are believed to remain after the Mo reaction analogous to that shown in eq. [3].

The X-ray crystal structure of **W**N=NH is shown in Fig. 6. Owing to the presence of two independent molecules in the unit cell and the difficulty of obtaining adequately sized crystals of this compound, the quality of this structure is mediocre (*R*1 = 10%). However, it was possible to refine all non-hydrogen atoms anisotropically. The critical geometrical parameters of the two crystallographically independent molecules are statistically indistinguishable (within 3σ). The average W—N_α (1.732(9) Å) and N_α—N_β (1.286(11) Å) distances are shorter and longer, respectively, than those in **Mo**N=NH (1.810(7) and 1.25(1) Å, Table 2), consistent with a greater degree of backbonding from tungsten into the N=NH group. A greater degree of backbonding from W is also evident from a lower value for ν(N-N) in **W**N=NH (1542 cm^{-1}) than in **Mo**N=NH (1587 cm^{-1}). Each molecule of **W**N=NH is noticeably asymmetric within the $[HIPTN_3N]^{3-}$ ligand. One W—N(amide) distance is slightly shorter than the other two in each molecule, and the HIPT group attached to that amido nitrogen is rotated out of its plane by an average of 68° in the direction *opposite* to the average turn of 28° found for the other two HIPT groups in each molecule. As a result, the three HIPT groups in each molecule do not form a pseudo three-fold symmetric propeller arrangement around the apical pocket similar to what is found in 13 other $[HIPTN_3N]$Mo and $[HIPTN_3N]$W derivatives. The hydrazide ligand is bent at both W (N5-W-N4 = 173.1(4)°) and N5 (W-N5-N6 = 173.6(9)°) in the same direction, primarily toward the unique N(amide) (N3A in the molecule shown in Fig. 6). The diazenide hydrogen was not located, but was added and refined in the position shown. It should be noted that N_α-N_β-R angles in diazenido compounds vary, e.g., from 132° in $[(Me_3SiNCH_2CH_2)_2NCH_2CH_2NMe_2)]$-$Mo(CH_3)(N_2TMS)$ to 170° in $\{[(Me_3SiNCH_2CH_2)_2N$-$CH_2CH_2NMe_2]Mo\text{-}N{=}NSiMe_3\}OTf$ (56). Therefore, we cannot say with any degree of certainty exactly where H_β is located. To our knowledge, **Mo**N=NH (33, 34) and **W**N=NH are the only structurally characterized examples of parent diazenide complexes of any metal.

Protonation of **W**N=NH at N_β with $[H(OEt)_2][BAr'_4]$ in ether affords the hydrazido(2–) species $[\mathbf{W}{=}NNH_2][BAr'_4]$ essentially quantitatively (eq. [4]). This W(VI) species can be isolated in good yield as a pale-yellow solid and has been fully characterized. The $NNH_2{}^+$ resonance appears at 5.96 ppm in the ^1H NMR spectrum in C_6D_6, flanked by barely resolved ^{183}W satellites ($^1J(^{183}W\text{-}H)$ = 6 Hz). Labeled $[\mathbf{W}{=}^{15}N^{15}NH_2][BAr'_4]$ features a doublet of doublets for the $^{15}N^{15}NH_2{}^+$ resonance in the ^1H NMR spectrum ($^1J(^{15}N_\beta\text{-}H)$ = 83.6 Hz, $^2J(^{15}N_\alpha\text{-}H)$ = 1.8 Hz) and a doublet at 344 ($^{15}N_\alpha\text{-}^{15}N_\beta H_2{}^+$) and a triplet of doublets at 131 ppm ($^{15}N_\alpha\text{-}^{15}N_\beta H_2{}^+$, $J(^{15}N\text{-}^{15}N)$ = 10.1 Hz) in the ^{15}N NMR spectrum. While the spectra of $[\mathbf{W}{=}NNH_2][BAr'_4]$ are generally similar to those of $[\mathbf{Mo}{=}NNH_2][BAr'_4]$, ^{15}N NMR data for $[\mathbf{W}{=}NNH_2][BAr'_4]$ reveal a reduction of $^1J(^{15}N_\beta\text{-}H)$ to 83.6 Hz in $[\mathbf{W}{=}NNH_2][BAr'_4]$ from 90.5 Hz in $[\mathbf{Mo}{=}NNH_2]$-$[BAr'_4]$ (34), consistent with an increased *p* character in the bonding at N_β as a consequence of a greater degree of backbonding to the NNH_2 unit in $[\mathbf{W}{=}NNH_2][BAr'_4]$.

The structure of $[\mathbf{W}{=}NNH_2][BAr'_4]$ (Fig. 7) is similar to other $\{[HIPTN_3N]M\}[BAr'_4]$ (M = Mo, W) derivatives that have been characterized in an X-ray study. The N_α—N_β distance (1.315(5) Å) is essentially identical to that in

[3] $\mathbf{W}\text{-N=NK} \xrightarrow{1.0[Et_3NH][OTf],\ C_6H_6}$

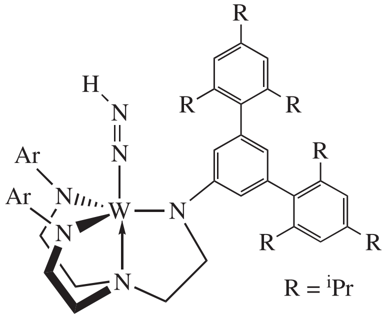

W-N=NH, 55%

Fig. 6. Thermal ellipsoid drawing of **W**-N=NH (50% probability level, selected hydrogen atoms omitted).

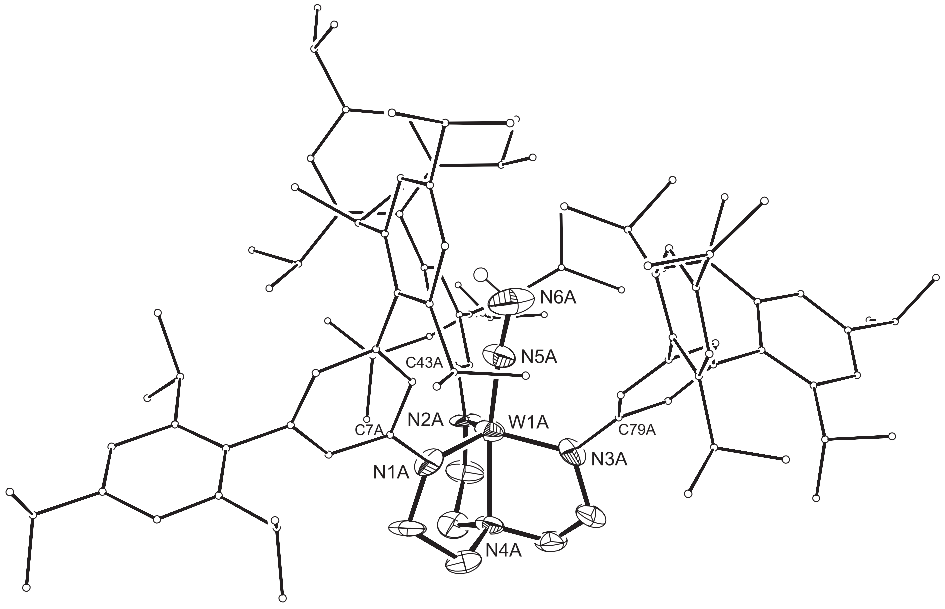

[4]

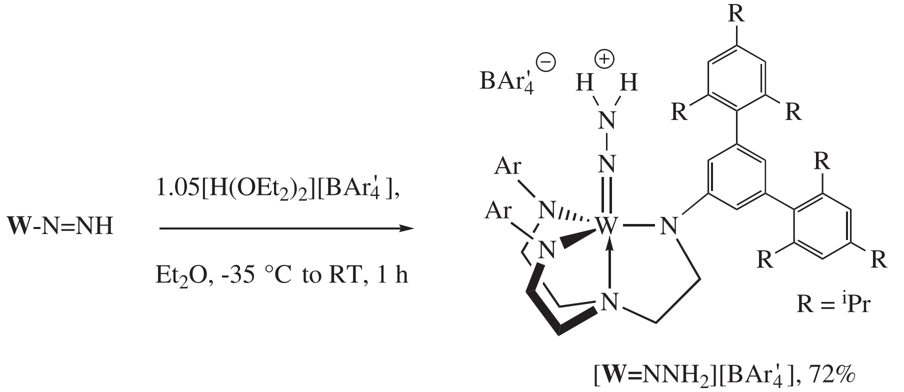

[**Mo**=NNH$_2$][BAr$'_4$] (1.310(5) Å). Since the N$_\alpha$—N$_\beta$ distance in [**W**=NNH$_2$][BAr$'_4$] is similar to that in **W**N=NH (1.29(1) Å), the amount of N$_\alpha$—N$_\beta$ double bond character must be significant, as one would expect in a M-N-N π system of this type. The NNH$_2^+$ hydrogens were not located, but were refined in calculated positions. Regardless of the particular orientation chosen for their representation, their presence in the model had a slight, but constant, effect on the refined N—N distance.

Electrochemical reduction of [**W**=NNH$_2$][BAr$'_4$] in 0.1 mol/L [Bu$_4$N][BAr$'_4$]/PhF at a glassy carbon electrode is irreversible at scan rates of up to 1 V/s and takes place at I_{pc} = –2.2 V vs. FeCp$_2^{+/0}$ (100 mV/s scan rate). The **Mo** analog, [**Mo**=NNH$_2$][BAr$'_4$], undergoes a quasi-reversible reduction at –1.56 V under the same conditions (34), which allows us to estimate the difference between the **Mo**=NNH$_2^{+/0}$ and **W**=NNH$_2^{+/0}$ couples as being 400–500 mV. The magnitude of this difference is considerably greater than that found for [**M**N$_2$]$^{0/-}$ (260 mV) and [**M**N$_2$]$^{+/0}$ (0 mV) potentials (M = Mo or W, vide supra). Apparently π donation of electron density from M into the [NNH$_2$]$^{2-}$ system does not differ substantially for Mo and W, and the **M**=NNH$_2^{+/0}$ potential difference therefore better reflects the difference in the HOMO energy that results from substitution of W for Mo alone. Consistent with this hypothesis, a large difference between Mo and W is also found for the **M**(NH$_3$)$^{+/0}$ potentials (vide infra).

Synthesis of [W(NH$_3$)][BAr$'_4$], its structure, and reactivity

When **W**Cl is treated with NaBAr$'_4$ and NH$_3$ in PhF [**W**(NH$_3$)][BAr$'_4$] is formed nearly quantitatively (eq. [5]). This reactivity mirrors that established for **Mo**Cl (33), except that fluorobenzene had to be used as a solvent because **W**Cl was found to be incompatible with dichloromethane. The ammonia adduct was isolated in good yield and fully characterized. Its ^{1}H NMR spectrum in C$_6$D$_6$ features a pattern of paramagnetically shifted and broadened resonances characteristic of a high-spin d^2 **W** environment in complexes of this general type. The resonances in **W**(NH$_3$)$^+$ are paramagnetically shifted to a greater extent than those of **W**Cl, a phenomenon that was also observed for **Mo**(NH$_3$)$^+$ vs. **Mo**Cl.

Fig. 7. Thermal ellipsoid drawing of [**W**=NNH_2][BAr'_4] (50% probability level, selected hydrogen atoms omitted).

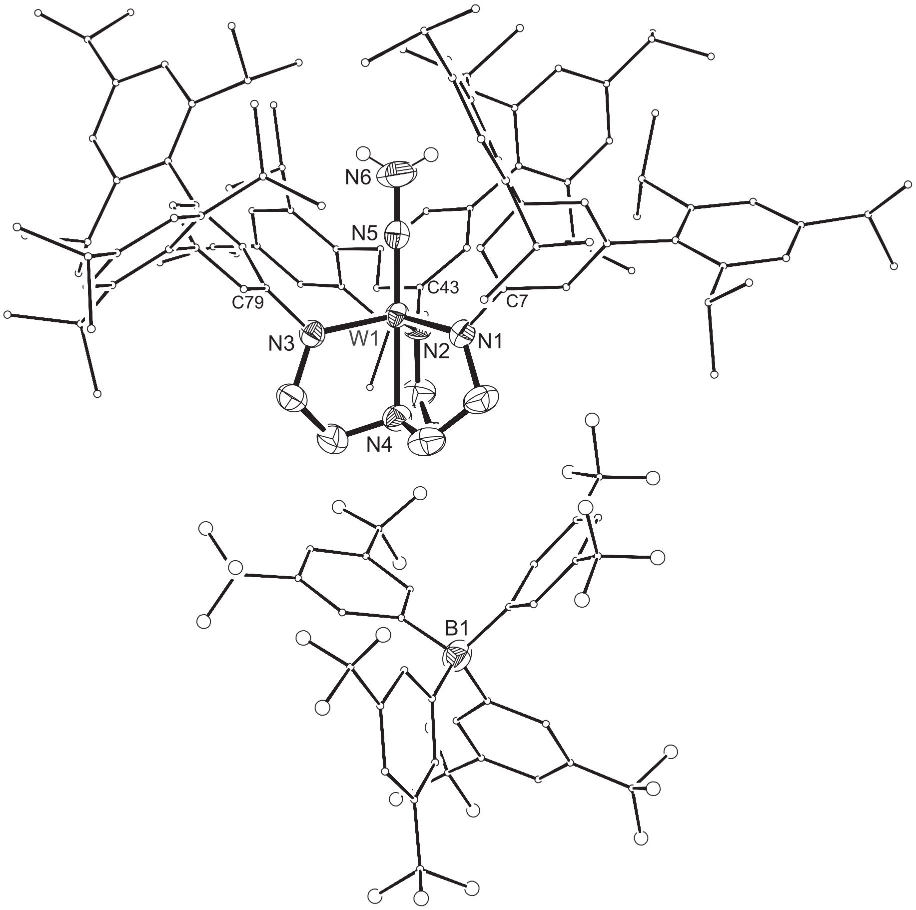

[5]

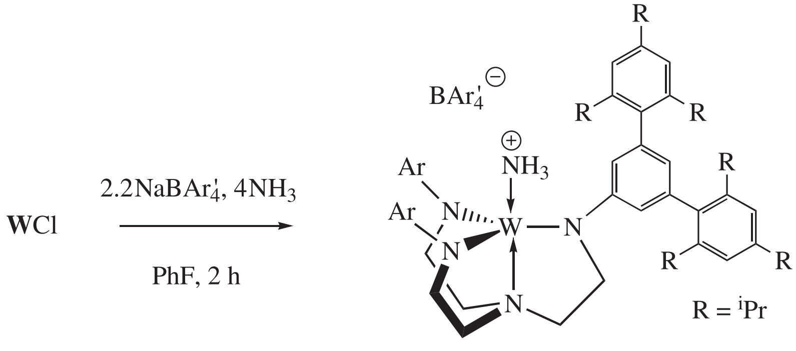

[**W**(NH_3)][BAr'_4], 87%

The X-ray crystal structure of [**W**(NH_3)][BAr'_4] (Fig. 8) is essentially identical to that of [**Mo**(NH_3)][BAr'_4] (33). The M—N(ammonia) distances are 2.210(4) Å in [**W**(NH_3)][BAr'_4] vs. 2.24(1) Å in [**Mo**(NH_3)][BAr'_4] (Table 2). The ammonia protons were not located, but are shown in calculated positions.

Electrochemical reduction of [**W**(NH_3)][BAr'_4] in 0.1 mol/L [Bu_4N][BAr'_4]/PhF at a glassy carbon electrode reveals an irreversible wave at a scan rate of 0.5 V/s (Fig. 9). The couple appears to become more reversible at faster scan rates (1 and 2 V/s) at –2.06 V vs. $FeCp_2^{+/0}$, although it cannot be called reversible even at 2 V/s. In contrast, one-electron reduction of [**Mo**(NH_3)][BAr'_4] is fully reversible both in PhF (0.1 mol/L [Bu_4N][BAr'_4]) at a glassy carbon electrode and THF (0.4 mol/L [Bu_4N][PF_6]) at a platinum disk at all scan rates and takes place at $E^{\circ\prime}$(**Mo**$(NH_3)^{+/0}$) = –1.63 V vs. $FeCp_2^{+/0}$ in PhF (0.1 mol/L [Bu_4N][BAr'_4]). The difference in **M**$(NH_3)^{+/0}$ potentials (M = Mo or W) is thus ~430 mV, similar to the difference between the **Mo**=$NNH_2^{+/0}$ and **W**=$NNH_2^{+/0}$ potentials (vide supra). Chemical reductions of both [**W**=NNH_2][BAr'_4] and [**W**(NH_3)][BAr'_4] are described below.

Deprotonation of [**W**(NH_3)]$^+$ with LiN$(SiMe_3)_2$/4TMEDA in C_6D_6 yields a single paramagnetic product, which we pre-

Fig. 8. Thermal ellipsoid drawing of [**W**(NH_3)][BAr'_4] (50% probability level, selected hydrogen atoms omitted).

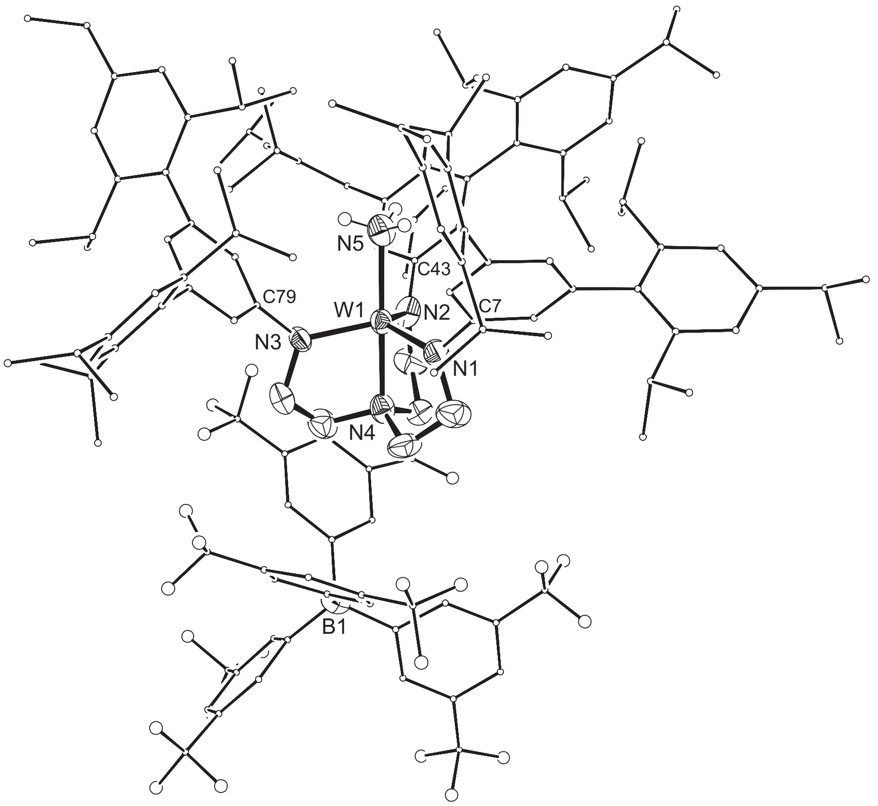

[6]

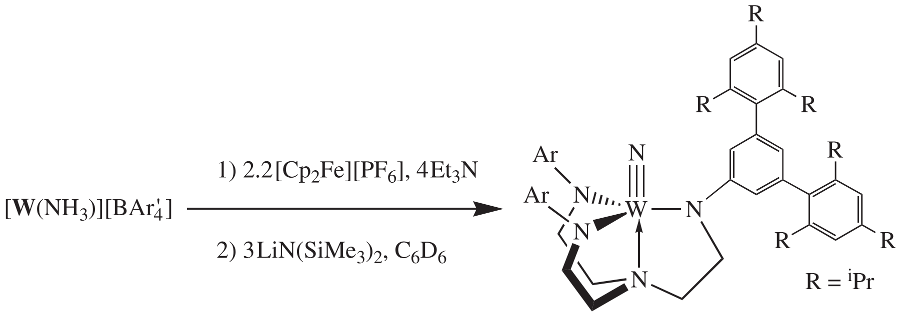

W≡N

sume to be (at least initially) **W**(NH_2). However, attempts to isolate the product in analytically pure crystalline form so far have failed. Treatment of [**W**(NH_3)][BAr'_4] with triethylamine and [$FeCp_2$][PF_6] in C_6D_6, followed by LiN($SiMe_3$)$_2$ yielded **W**≡N essentially quantitatively (eq. [6]). The nitride can be prepared more conveniently via salt metathesis of **W**Cl with 3 equiv. of NaN_3 in a mixture of C_6H_6 and MeCN over a period of 16 h at room temperature (eq. [7]), the method utilized originally in the synthesis of [Me_3SiN_3N]W≡N (42). The IR spectra of **W**≡N and **Mo**≡N in C_6D_6 are virtually identical in the 1200–900 cm^{-1} region, with the exception of an absorption at 1012 cm^{-1} in the **Mo**≡N spectrum (ν(Mo-N)) and at 1024 cm^{-1} in the **W**≡N spectrum. Therefore, we assign the 1024 cm^{-1} absorption to the ν(W-N) stretch. As in [Me_3SiN_3N]M≡N complexes, ν(M-N) is slightly higher for **W**≡N than it is in **Mo**≡N. The ^{15}N NMR spectrum of **W**≡^{15}N shows a resonance for the nitride at 827 ppm (vs. 898 ppm in **Mo**≡^{15}N).

[7] $$\mathbf{W}\text{Cl} \xrightarrow[\text{16 h, RT, 58\%}]{3NaN_3,\ C_6H_6\text{: MeCN,}} \mathbf{W}\equiv\text{N}$$

Treatment of a C_6D_6 solution of [**W**(NH_3)][BAr'_4] with $LiBHEt_3$ (1 mol/L in THF) results in a color change to brown and formation of a largely one paramagnetic species, which is tentatively assigned as the monohydride complex, **W**H, on the basis of reactivity similar to that exhibited by **Mo**H (33). However, a small amount of a diamagnetic product is present initially, which becomes the sole observable species when the reaction mixture is exposed to an atmosphere of H_2 for ~10 min (eq. [8]); this diamagnetic species (**W**H_3) can be isolated in 42% yield. This compound was identified on the basis of the similarity of its NMR and IR spectra with those of the crystallographically characterized

[8]
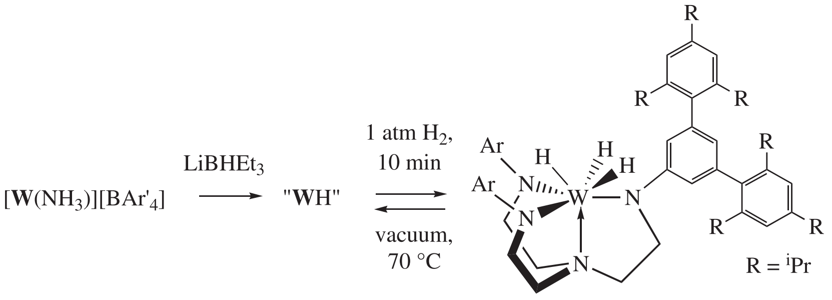

WH₃

Fig. 9. Electrochemical behavior of [**W**(NH_3)][BAr$'_4$] in 0.1 mol/L [Bu_4N][BAr$'_4$]/PhF, recorded at a glassy carbon electrode (3 mm diam.) at the scan rates shown in V/s. The potential scale is referenced to $FeCp_2^{+/0}$.

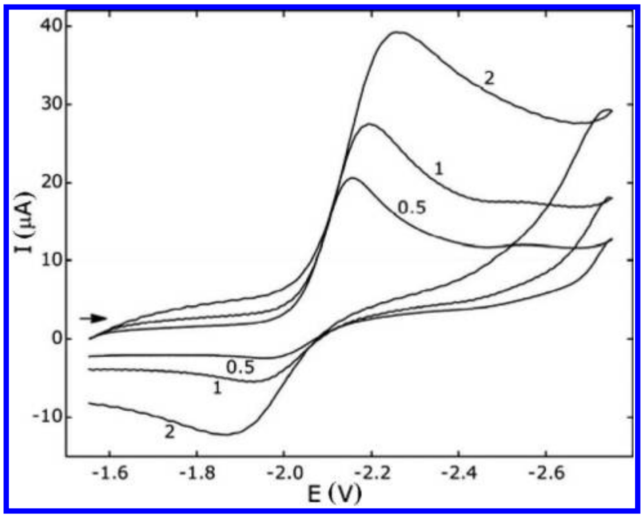

complex, [Me_3SiN_3N]WH_3 (57). Like [Me_3SiN_3N]WH_3, **W**H_3 features a low-field resonance of intensity three in its ^1H NMR spectrum in C_6D_6 at 11.99 ppm with $^1J(^{183}W\text{-}H)$ = 24 Hz (cf. 10.01 ppm and 23 Hz in [Me_3SiN_3N]WH_3), in addition to characteristic ligand resonances. The IR spectrum of **W**H_3 in C_6D_6 shows two broad absorptions at 1958 and 1966 cm^{-1} consistent with ν(W-H) stretching modes (cf. 1903 and 1887 cm^{-1} in [Me_3SiN_3N]WH_3 in Nujol). However, unlike [Me_3SiN_3N]WH_3, **W**H_3 can be induced to lose H_2, by exposure to a high vacuum at 70 °C to yield a mixture that contains a considerable amount of **W**H after a few hours. This difference in behavior can be attributed to less electron donation by the [$HIPTN_3N$]$^{3-}$ ligand compared to the [Me_3SiN_3N]$^{3-}$ ligand. It should be noted that what is proposed to be [$HIPTN_3N$]MoH_3 cannot be isolated since it readily loses dihydrogen to form [$HIPTN_3N$]MoH at room temperature (34).

Reduction of dinitrogen on W with protons and electrons

Treatment of **W**N_2 with 1 equiv. of [2,6-LutH][BAr$'_4$] (2,6-Lut = 2,6-lutidine) and 2 equiv. of $CoCp_2$ in C_6D_6 results in a subtle color change, formation of a yellow precipitate of [$CoCp_2$][BAr$'_4$], complete consumption of the acid, and conversion of approximately half of the starting **W**N_2 to [**W**=NNH_2][BAr$'_4$] in 3 h at 22 °C (eq. [9]). This mixture remains unchanged over a period of 24 h. **W**N=NH is converted quantitatively into [**W**=NNH_2][BAr$'_4$] upon reaction with 1 equiv. of [2,6-LutH][BAr$'_4$] in C_6D_6. Therefore, we propose that **W**N=NH is formed in the reduction of **W**N_2 in the presence of [2,6-LutH][BAr$'_4$] and that **W**N=NH then consumes a proton relatively irreversibly to give [**W**=NNH_2][BAr$'_4$], thereby limiting consumption of **W**N_2 when 1 equiv. of acid is present to ~50%. In contrast, the analogous reaction between **Mo**N_2 and [2,6-LutH][BAr$'_4$] and $CoCp_2$ rapidly yields **Mo**N=NH quantitatively (34). [**Mo**=NNH_2][BAr$'_4$] is considerably more acidic than [**W**=NNH_2][BAr$'_4$], as judged from the fact that treatment of **Mo**N=NH with 1 equiv. of [2,6-LutH][BAr$'_4$] in C_6D_6 gives an equilibrium mixture of **Mo**N=NH and [**Mo**=NNH_2][BAr$'_4$] (44:56); therefore, conversion of **Mo**N_2 to **Mo**N=NH can be complete when **Mo**N_2 is treated with only 1 equiv. of [2,6-LutH][BAr$'_4$] and $CoCp_2$. The most important point is that a one-electron reduction–protonation of **W**N_2 to yield **W**N=NH is feasible, although this process appears to be slower than conversion of **Mo**N_2 to **Mo**N=NH under analogous conditions.

Isolated [**W**=NNH_2][BAr$'_4$] reacts rapidly with 2 equiv. of $CoCp_2^*$ ($E°'$ = –2.01 V vs. $FeCp_2^{+/0}$ in PhF) in C_6D_6, as indicated by the formation of a yellow precipitate of [$CoCp_2^*$][BAr$'_4$]. However, instead of the expected one-electron reduced (W(V)) product (**W**=NNH_2), a proton NMR spectrum of the reaction mixture recorded 20 min after mixing [**W**=NNH_2][BAr$'_4$] and $CoCp_2^*$ revealed that only **W**N=NH and **W**≡N were present in a 52:48 ratio. After 17 h, the ratio of **W**N=NH to **W**≡N had not changed, but a well-resolved triplet for free ammonia could be observed. This ammonia was collected by vacuum transfer and shown (using the indophenol analytical method) to amount to 0.43 equiv. of the original [**W**=NNH_2][BAr$'_4$]. Therefore, one-electron reduction of [**W**=NNH_2][BAr$'_4$] predominantly results in the net reaction shown in eq. [10]. In fact, this reaction was used to prepare **W**≡^{15}N from [**W**=$^{15}N^{15}NH_2$][BAr$'_4$]. This stoichiometry is consistent with the disproportionation of the initial reduction product, **W**=NNH_2, a W(V) species, into a W(IV) and a W(VI) species, **W**N=NH and **W**≡N, respectively. A plausible sequence of elementary electron- and

[9]
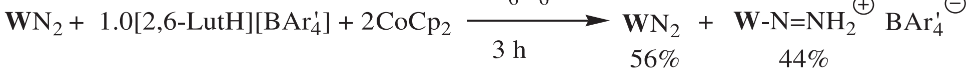

$$\mathbf{W}N_2 + 1.0[2,6\text{-LutH}][BAr'_4] + 2CoCp_2 \xrightarrow[3\ h]{C_6D_6} \underset{56\%}{\mathbf{W}N_2} + \underset{44\%}{\mathbf{W}\text{-}N{=}NH_2^{\oplus}}\ BAr_4'^{\ominus}$$

Scheme 1. A proposed sequence of reactions that yields the net process shown in eq. [10]. Unobservable intermediates are shown in boxes. The counterion ($BAr'_4{}^-$) is excluded for clarity. PT = proton transfer, ET = electron transfer.

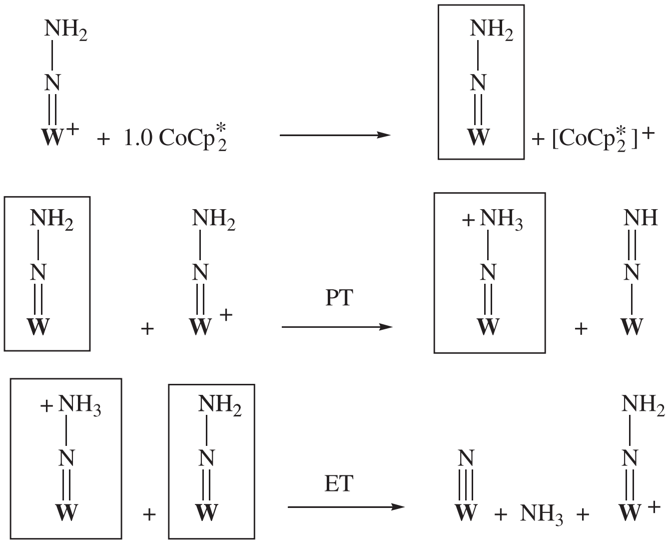

proton-transfer steps that comprises the overall process is proposed in Scheme 1.

$$[10]\quad [\mathbf{W}\text{=N-NH}_2]\text{BAr}'_4 + 1.0\text{CoCp}^*_2 \xrightarrow{C_6D_6} 0.5\mathbf{W}\text{-N=NH} + 0.5\mathbf{W}\equiv\text{N} + 0.5\,\text{NH}_3 + [\text{CoCp}^*_2]\text{BAr}'_4$$

Initial one-electron reduction of **W**=$NNH_2{}^+$ yields as yet unobserved **W**=NNH_2, possibly in a rapid equilibrium. A small amount of **W**=$NNH_2{}^+$ then protonates **W**=NNH_2 to yield the proposed hydrazidium(2–) species (**W**=$NNH_3{}^+$), while **W**=$NNH_2{}^+$ is transformed into **W**N=NH. The hydrazidium(2–) species (**W**=$NNH_3{}^+$) then oxidizes **W**=NNH_2 to regenerate **W**=$NNH_2{}^+$, and in the process is reduced to form **W**≡N and ammonia. Essentially, the disproportionation of **W**=NNH_2 is catalyzed by **W**=$NNH_2{}^+$.

It is possible that the disproportionation shown in Scheme 1 requires some time to proceed to completion and that the initial "**W**(V) = NNH_2" exists in a fast electron-transfer equilibrium with **W**=$NNH_2{}^+$ and (or) $CoCp^{*+}_2$, which causes extensive broadening and (or) complete disappearance of the resonances for **W**=$NNH_2{}^+$ and $CoCp^{*+}_2$ in the ^{1}H NMR spectrum. A similar situation was encountered in the reversible reduction of{[$HTBTN_3N$]Mo(NH_3)}[BAr'_4] with $CrCp^*_2$ in C_6D_6 (37). However, irreversibility of the electrochemical reduction of [**W**=NNH_2][BAr'_4] suggests that the sequence of reactions following the initial electron transfer takes place rapidly at 22 °C. We are puzzled by the apparently fast rate of net proton transfer in the absence of conspicuous proton-transfer mediators. However, we note that small amounts of the free ligand, H_3[$HIPTN_3N$], are typically formed in a decomposition reaction, and could easily mediate the proton-transfer step. The actual mechanism of the proton-transfer step remains to be clarified.

Reduction of [**Mo**=NNH_2][BAr'_4] at room temperature proceeds in a manner closely analogous to that shown in eq. [10] and (it is proposed) Scheme 1 (34). One of the reasons to investigate the chemistry of [**W**=NNH_2][BAr'_4] was the possibility that **W**=NNH_2 would be more stable than **Mo**=NNH_2 and that **W**=NNH_2, therefore, could at least be observed. Instead, however, we find that **W**=NNH_2 is even less stable than **Mo**=NNH_2. In each case, the high propensity of **M**=NNH_2 to disproportionate can be attributed to a combination of a high Brønsted basicity of N_β in combination with strong reducing properties. We attribute the strong reducing properties to the presence of one of the five electrons in the M-N_α-N_β π system in a π orbital that has a node at N_α; four electrons are in the two perpendicular lowest energy bonding molecular orbitals. This combination of properties makes **M**=NNH_2 susceptible to *both* protonation by its own oxidized form *and* oxidation by its own protonated form, at least in a thermodynamic sense. If both steps are kinetically feasible, then disproportionation proceeds readily, perhaps in part because of the fact that the step in which ammonia is formed (N—N bond cleavage) is almost certainly irreversible. It is important to note that disproportionation of **M**=NNH_2 intermediates has no adverse consequences for overall reduction of dinitrogen to ammonia, since it merely leads to species that are themselves susceptible to further reactions that lead to the formation of ammonia. Disproportionations of d^1 species and related intermolecular proton or electron transfer reactions are likely to complicate the mechanism of ammonia formation depicted in Fig. 2, when all species are in solution.

Attempted conversion of W(NH_3)$^+$ to WN_2, and catalytic reduction of N_2

The results discussed in the previous section show that it is possible to reduce **W**N_2 to yield ammonia and **W**≡N in the presence of acid and reductant. Since reduction of **Mo**≡N to **Mo**(NH_3)$^+$ is a relatively easy transformation in the **Mo** dinitrogen reduction cycle (35), while reduction of **Mo**(NH_3)$^+$ to **Mo**(NH_3) and transformation of **Mo**(NH_3) into **Mo**N_2 can be observed (34), we examined the feasibility of converting **W**(NH_3)$^+$ into **W**N_2.

Reduction of [**W**(NH_3)][BAr'_4] with 2 equiv. of $CoCp^*_2$ in C_6D_6 proceeds to some extent, as judged by the rapid formation of a yellow precipitate of [$CoCp^*_2$][BAr'_4]. However, the ^{1}H NMR spectrum of the resulting solution is unusually featureless, i.e., few resonances beyond isopropyl methyl resonances and some aryl resonances can be observed. Since the ^{1}H NMR spectrum of **Mo**(NH_3) is similar to that of other d^3 Mo complexes in this general family, we expected **W**(NH_3) to be observable and to have a very similar spectrum to that of **Mo**(NH_3).

The mixture of [**W**(NH_3)][BAr'_4] and **W**(NH_3) remained unchanged for days and also did not change after being exposed to 800 psi (1 psi = 6.894 757 kPa) of N_2 for 48 h. Thermolysis at 60 °C for a day resulted only in minor decomposition and formation of **W**≡N and **W**H_3. Treatment of **W**N_2 with ~4 equiv. of NH_3 in C_6D_6 under argon also resulted in no change after 15 days, again in sharp contrast to the behavior in the analogous molybdenum system where an equilibrium between **Mo**(NH_3) into **Mo**N_2 is readily established in a closed system over a period of several hours. Although it has not been possible to transform **W**(NH_3) into **W**N_2, **W**(NH_3) appears to be relatively stable, at least as

Table 3. Results of the attempted catalytic reduction of dinitrogen with $\mathbf{W}N_2$.[a]

Reductant	$E^{\circ\prime}$(THF)[b]	$E^{\circ\prime}$(PhF)[c]	Acid	pK_a (H_2O)	Equiv. of NH_3[d]
$CrCp^*_2$	–1.47	–1.63	[2,6-LutH][BAr'_4]	6.68	1.31
$CoCp^*_2$	–1.84	–2.01	[2,6-LutH][BAr'_4]	6.68	1.51
$CoCp^*_2$	–1.84	–2.01	[Et_3NH][BAr'_4]	10.67	0.62

[a] Single runs of all experiments were carried out with 5.84 μmol of $\mathbf{W}N_2$, 36 equiv. of the reductant, and 48 equiv. of the acid, under conditions otherwise identical to those previously described (35, 37).

[b] V vs. $FeCp_2^{+/0}$ in 0.4 mol/L [Bu_4N][PF_6].

[c] V vs. $FeCp_2^{+/0}$ in 0.1 mol/L [Bu_4N][BAr'_4].

[d] The maximum possible is 12 equiv. of ammonia (36 electrons available).

generated by reduction of [$\mathbf{W}(NH_3)$][BAr'_4] with $CoCp^*_2$. However, this conclusion is difficult to reconcile with a limited degree of reversibility of the electrochemical reduction of [$\mathbf{W}(NH_3)$][BAr'_4] ([Bu_4N][BAr'_4]/PhF) (Fig. 9). Therefore, the exact nature of the putative "$\mathbf{W}(NH_3)$" remains obscure, and we cannot exclude the possibility that some reaction involving oxidation of W(III) (e.g., intramolecular NH addition) is facile. In any case, it seems likely that $\mathbf{W}(NH_3)$ is not strictly analogous to well-behaved $\mathbf{Mo}(NH_3)$ (34).

Treatment of the mixture containing partly reduced $\mathbf{W}(NH_3)^+$ in C_6D_6 with [Et_3NH][BAr'_4] produced a new paramagnetic species that gave rise to considerable quantities of both $\mathbf{W}(NH_3)^+$ and $\mathbf{W}H_3$ after several days, but no $\mathbf{W}N_2$ or products of its reduction. The net reaction of $\mathbf{W}(NH_3)^+$ with a reductant and an acid thus results primarily in reduction of protons (presumably) and formation (ultimately) of $\mathbf{W}H_3$ (eq. [11]), but dinitrogen is not bound or reduced.

$$[11] \quad [\mathbf{W}(NH_3)][BAr'_4] + 4CoCp^*_2 + 3[Et_3NH][BAr'_4] \longrightarrow \mathbf{W}H_3 + NH_3 + 4[CoCp^*_2][BAr'_4] + 3Et_3N$$

In view of the previous observations, it is perhaps not surprising that attempted catalytic reduction of dinitrogen using $\mathbf{W}N_2$ as the catalyst under conditions identical or similar to those employed for catalytic reduction of dinitrogen by Mo complexes (35) failed (Table 3). This can be attributed chiefly to the inability to convert $\mathbf{W}(NH_3)^+$ into $\mathbf{W}N_2$ to any significant extent on the timescale of a typical catalytic experiment (6 h), as was independently established in the experiments previously described. Ammonia is formed, but less than 2 equiv., i.e., at most 1.51 equiv. with $CoCp^*_2$ as the reductant and [2,6-LutH][BAr'_4] as the acid. Therefore, while it is possible to cleave the N—N bond and form the first equivalent of ammonia, and to form some $\mathbf{W}NH_x^{y+}$ species that yield additional ammonia upon workup, dinitrogen is not bound and reduced further under the conditions employed.

Conclusions

We have been able to synthesize a number of [$HIPTN_3N$]W complexes analogous to the [$HIPTN_3N$]Mo species that are proposed intermediates in the catalytic reduction of dinitrogen to ammonia (35), among them the first terminal dinitrogen complex of W(III) ($\mathbf{W}N_2$), the second structurally characterized example of a parent diazenide of any metal ($\mathbf{W}N{=}NH$), and three other tungsten derivatives containing dinitrogen at various stages of reduction ($\mathbf{W}N{=}NH_2^+$, $\mathbf{W}{\equiv}N$, and $\mathbf{W}(NH_3)^+$). As expected, tungsten variants of known molybdenum complexes are characterized by greater nucleophilicities (at N_β) and lower reduction potentials. Interestingly, however, the differences between Mo and W potentials are considerably less pronounced for complexes that contain a dinitrogen ligand, e.g., 260 mV for $\mathbf{M}N_2^{0/-}$ and 0 mV for $\mathbf{M}N_2^{+/0}$. Structural and spectroscopic data (Table 2) signify the more electron-rich nature of all other tungsten derivatives without exception. We had hoped to observe and possibly isolate W variants of several proposed Mo species that are either exceedingly difficult to isolate, and in some cases even observe in situ. However, many of the W complexes, e.g., [$\mathbf{W}N_2$][Bu_4N] and $\mathbf{W}(NH_3)$, were in fact less stable than the analogous Mo complexes. Also $\mathbf{W}{=}NNH_2$ disproportionates into a mixture of $\mathbf{W}N{=}NH$, $\mathbf{W}{\equiv}N$, and ammonia much faster than does $\mathbf{Mo}{=}NNH_2$. Although dinitrogen in $\mathbf{W}N_2$ could be reduced to ammonia with acid and reductant combinations similar to those used in the catalytic reduction of dinitrogen with [$HIPTN_3N$]Mo species, catalytic turnover could not be achieved as a consequence of (inter alia) major difficulties in converting $\mathbf{W}(NH_3)^+$ into $\mathbf{W}N_2$. Complications of this magnitude in a system where Mo analogs are intermediates in the catalytic reduction of dinitrogen to ammonia would appear to doom tungsten as a plausible site for dinitrogen reduction. *If* MoFe and WFe nitrogenases are structurally analogous, and *if* dinitrogen is reduced at Mo in the MoFe nitrogenase, then one can imagine why reduction of dinitrogen by the WFe nitrogenase might fail.

Experimental section

General

All air- and moisture-sensitive compounds were manipulated using standard Schlenk and glovebox techniques under an atmosphere of nitrogen in flame- and oven-dried glassware (including NMR tubes). Ether, pentane, and toluene were purged with nitrogen, passed through activated alumina columns (58), and freeze–pump–thaw degassed three times. THF, DME, 1,4-dioxane, and benzene were distilled from dark purple Na–benzophenone ketyl solutions. Dichloromethane and acetonitrile were distilled from CaH_2, while fluorobenzene was distilled from P_2O_5 under N_2. All dried and deoxygenated solvents were stored over molecular sieves in a nitrogen-filled glovebox. Small quantities of hydrocarbon and ether solvents, as well as all such deuterated NMR solvents, were purified a second time by vacuum transfer from dark-purple solutions and (or) suspensions of Na–benzophenone ketyl (or CaH_2 for CH_2Cl_2, PhF, and

CD_2Cl_2), degassed, and stored in gas-tight solvent bulbs inside a glovebox. Molecular sieves (3 Å) and Celite® were activated in vacuo at 230 °C for several days. Cobaltocene (sublimed), $CrCp^*_2$ (sublimed), $[CoCp^*_2][PF_6]$ (Strem), $(Me_3Si)_2NLi$ (sublimed), anhydr. $ZnCl_2$, $LiBHEt_3$ (1 mol/L THF), and NaN_3 (Aldrich) were used as received, unless indicated otherwise. $WCl_4(DME)$ (59), $H_3[HIPTN_3N]$ (33), $NaBAr'_4$ (60), $[H(OEt_2)_2][BAr'_4]$ (60), and [2,6-LutH]$[BAr'_4]$ (35) were prepared according to the published procedures or slight modifications thereof. Potassium graphite (KC_8) was prepared by stirring potassium metal, freshly cut in a nitrogen-filled glovebox, and graphite in 1:8 stoichiometry with a glass-coated stirbar under 700 torr (1 torr = 133.322 Pa) of Ar at 140 °C for an hour. $CoCp^*_2$ was prepared from $[CoCp^*_2][PF_6]$ and a slight excess of KC_8 in THF over 4 h and sublimed. $[Et_3NH][BAr'_4]$ was prepared from Et_3NHCl and 1.05 equiv. of $NaBAr'_4$ in CH_2Cl_2. All metal complexes were stored in the dark, under N_2 at –35 °C. ^1H, ^{19}F, and ^{15}N NMR spectra were recorded on a Varian Mercury 300 (^1H 300 MHz, ^{19}F 282 MHz), Varian Unity 300 (^1H 300 MHz) or a Varian Inova 500 (^1H 500 MHz, ^{15}N 50.7 MHz) spectrometers and referenced to the residual protio solvent peaks (^1H) or external neat PhF (^{19}F, –113.15 ppm relative to $CFCl_3$) and neat MeCN (^{15}N, +245.5 ppm relative to neat NH_3 at 303 K (61)). Attempted catalytic dinitrogen reduction runs and analyses of ammonia by the indophenol method (62–65) utilized procedures, equipment, and reagents described previously (35, 37). IR spectra were recorded on a Nicolet Avatar 360 FT-IR spectrometer in 0.2 mm KBr solution cells; frequencies are given in cm^{-1}. Elemental analyses were performed by H. Kolbe Mikroanalytisches Laboratorium, Mülheim an der Ruhr, Germany.

Electrochemistry

Electrochemical measurements were carried out using a BAS CV-50W potentiostat, 0.1 mol/L $[Bu_4N][BAr'_4]$ in PhF electrolyte, and a standard three-electrode cell assembly with glassy carbon (3.0 mm diam.) disk working electrode, platinum wire auxiliary electrode, and a AgCl-coated silver wire reference electrode. All measurements were referenced internally with $FeCp_2$, $CoCp_2$, or **Mo**N_2 (35), as appropriate. Compensation of internal solution resistance was used to lower the peak separation of reversible couples to 100–200 mV using the standard routines available with the BAS CV-50W potentiostat and accompanying software. An explanation of the technique can be found on the web at http://www.epsilon-web.net/Ec/manual/Setup/ir_comp.html.

$[HIPTN_3N]WCl$

A mixture of $WCl_4(DME)$ (3.897 g, 9.37 mmol) and $H_3[HIPTN_3N]$ (14.93 g, 9.40 mmol) was stirred vigorously in benzene (100 mL) for 2 h to give a dark red-brown homogeneous solution. Solid $(Me_3Si)_2NLi$ (4.868 g, 29.1 mmol) was added in portions over a period of 10 min. The solution was stirred for an additional 2 h and taken to dryness in vacuo. The residue was dried at 70 °C overnight and extracted with benzene. The extracts were filtered through Celite®, and the filtrates were concentrated and centrifuged in portions to remove residual LiCl. The resulting homogeneous solution was then taken to dryness in vacuo and the residue was heated at 85 °C for several hours. Trituration of the residue with pentane (60 mL) afforded a dark orange microcrystalline solid, which was collected by filtration on a glass frit after standing the mixture at –35 °C overnight, washed with cold pentane, and dried in vacuo at 85 °C for several hours. Yield: 11.28 g (6.25 mmol, 67%). ^1H NMR (C_6D_6, 20 °C) δ: 18.81 (s, 6H, 4′,6′-*H*), 7.49 (s, 12H, 3,5,3″,5″-*H*), 3.47 (br s, 12H, 2,6,2″,6″-C*H*Me$_2$), 3.18 (sept, J_{HH} = 6.6 Hz, 6H, 4,4″-C*H*Me$_2$), 2.98 (s, 3H, 2′-*H*), 1.58 (d, J_{HH} = 6.6 Hz, 36H, 4,4″-CH(C*H*$_3$)$_2$), 1.34 (s, 36H, 2,6,2″,6″-CH(C*H*$_3$)$_2$), 0.83 (br s, 36H, 2,6,2″,6″-CH(C*H*$_3$)$_2$), –27.06 (s, 6H, NC*H*$_2$), –50.1 (br s, 6H, NC*H*$_2$). Anal. calcd. for $C_{114}H_{159}ClN_4W$ (%): C 75.87, H 8.88, N 3.10, Cl 1.96; found: C 75.97, H 8.78, N 2.97, Cl 2.10.

$[HIPTN_3N]WN{=}NK$

A mixture of **W**Cl (500 mg, 0.277 mmol) and KC_8 (93.6 mg, 0.692 mmol) was stirred in benzene (6 mL) under 1 atm of N_2 (1 atm = 101.325 kPa) with a glass-coated magnetic stirbar for 42 h. The resulting dark maroon-red mixture was taken to dryness in vacuo and the solid residue was extracted with pentane. The pentane extracts were filtered through Celite® and concentrated to 5 mL; a black-red crystalline solid formed within in minutes. The mixture was kept at –35 °C for several days and the product was then collected on a frit, washed with cold pentane, and dried in vacuo at 35 °C for 2 h. Yield: 310 mg (0.169 mmol, 61%). IR (C_6D_6): 1745 ($\nu_{N\text{-}N}$). IR (pentane): 1747 ($\nu_{N\text{-}N}$). ^1H NMR (C_6D_6, 20 °C) δ: 7.54 (br s, 6H, 4′,6′-*H*), 7.16 (s, 12H, 3,5,3″,5″-*H*), 6.61 (s, 3H, 2′-*H*), 3.75 (br s, 6H, NC*H*$_2$), 3.42 (sept, J_{HH} = 6.8 Hz, 12H, 2,6,2″,6″-C*H*Me$_2$), 2.84 (br sept, J_{HH} = 6 Hz, 6H, 4,4″-C*H*Me$_2$), 1.93 (br s, 6H, NC*H*$_2$), 1.26 (d, J_{HH} = 6.5 Hz, 36H, 4,4″-CH(C*H*$_3$)$_2$), 1.24 (d, J_{HH} = 6.0 Hz, 36H, 2,6,2″,6″-CH(C*H*$_3$)$_2$), 1.2 (br sh, 36H, 2,6,2″,6″-CH(C*H*$_3$)$_2$). Anal. calcd. for $C_{114}H_{159}KN_6W$ (%): C 74.56, H 8.73, N 4.58; found: C 74.43, H 8.59, N 4.45.

X-ray quality crystals were obtained from a supersaturated heptane solution at room temperature.

$[HIPTN_3N]W^{15}N{=}^{15}NK$

A mixture of **W**Cl (500 mg, 0.277 mmol) and KC_8 (93.6 mg, 0.692 mmol) in benzene (6 mL), prepared under regular N_2 in a 25 mL flask fitted with a Teflon® valve, was freeze–pump–thaw degassed five times, pressurized to 1 atm (1 atm = 101.325 kPa) with $^{15}N_2$ purified with solid Na–Ph_2CO and stirred with a glass-coated magnetic stirbar for 50 h. A work-up procedure analogous to that used in the preparation of the unlabeled complex yielded 285 mg (0.155 mmol, 56%) of a black-red solid, identified by spectroscopic data as the labeled compound enriched with ^{15}N at the N_α and N_β diazenido sites to the extent of only 92% as a consequence of some initial reaction under $^{14}N_2$ to yield $[HIPTN_3N]W^{14}N{=}^{14}NK$. IR ($C_6D_6$): 1745 ($\nu_{14N-14N}$), 1688 ($\nu_{15N-15N}$). ^{15}N NMR (C_6D_6, 20 °C) δ: 356.6 (d, $J(^{15}N_\alpha\text{-}^{15}N_\beta)$ = 11.2 Hz, $^{15}N_\alpha$), 349.5 (d, $J(^{15}N_\alpha\text{-}^{15}N_\beta)$ = 11.2 Hz, $^{15}N_\beta$).

$[HIPTN_3N]WN_2$

A mixture of **W**Cl (500 mg, 0.277 mmol) and KC_8 (93.6 mg, 0.692 mmol) was stirred in benzene (6 mL) under 1 atm of N_2 (1 atm = 101.325 kPa) with a glass-coated magnetic stirbar for 42 h. The resulting mixture was filtered through Celite® and brought to dryness in vacuo. Solid $ZnCl_2$ (30.2 mg, 0.222 mmol) and THF (6 mL) were added to the residue. After stirring the solution for a few minutes, a dark orange-red solution and a precipitate of Zn metal formed. The mixture was taken to dryness in vacuo and heated to 75 °C for 2 h. The solid residue was extracted with pentane and the pentane extracts were filtered through Celite®. The extracts were taken to dryness in vacuo. Addition of Me_4Si (7 mL) to the solid residue led to the formation of a microcrystalline orange solid after 1 h. The mixture was kept at –35 °C for several days and the solid product was collected on a frit, washed with cold Me_4Si, and dried in vacuo at 75 °C for 2 h. Yield: 265 mg (0.147 mmol, 53%). IR (C_6D_6): 1888 ($\nu_{\text{N-N}}$). ^{1}H NMR (C_6D_6, 20 °C) δ: 35.2 (br s, 6H, NCH_2), 6.79 (s, 12H, 3,5,3″,5″-*H*), 2.83 (s, 6H, 4,4″-C*H*Me$_2$), 2.58 (br s, 36H, 2,6,2″,6″-CH(CH_3)$_2$), 1.29 (s, 36H, 4,4″-CH(CH_3)$_2$), 0.66 (s, 36H, 2,6,2″,6″-CH(CH_3)$_2$), –0.25 (s, 2H, 2′-*H*), –0.95 (s, 12H, 2,6,2″,6″-C*H*Me$_2$), –11.1 (br s, 6H, 4′,6′-*H*), –22.5 (br s, 6H, NCH_2). Anal. calcd. for $C_{114}H_{159}N_6W$ (%): C 76.18, H 8.92, N 4.68; found: C 75.93, H 9.08, N 4.57.

X-ray quality crystals were obtained from a supersaturated heptane solution at room temperature.

[HIPTN$_3$N]W(^{15}N$_2$)

A mixture of **W**^{15}N=^{15}NK (10 mg) and $ZnCl_2$ (0.6 mg, 0.8 equiv.) in THF (0.6 mL) was stirred for 10 min. The mixture was filtered through Celite® and the filtrate was taken to dryness in vacuo. The solid residue was dissolved in C_6D_6 for spectroscopic analysis. IR (C_6D_6): 1888 ($\nu_{\text{14N–14N}}$), 1826 ($\nu_{\text{15N–15N}}$).

[HIPTN$_3$N]WN=NH

A mixture of **W**Cl (500 mg, 0.277 mmol) and KC_8 (93.6 mg, 0.692 mmol) was stirred in benzene (6 mL) with a glass-coated magnetic stirbar for 42 h under 1 atm of N_2 (1 atm = 101.325 kPa). The resulting dark maroon-red mixture was treated with solid [Et$_3$NH][OTf] (69.6 mg, 0.277 mmol), stirred for 30 min, and taken to dryness in vacuo. The solid residue was extracted with pentane and the pentane extracts were filtered through Celite®. Upon concentration of this solution to ~5 mL, the product precipitated as a cotton-like solid. Repeated warming and cooling of the mixture to –35 °C induced crystallization of the product in the form of a microcrystalline solid sufficiently dense to allow isolation by filtration. The resulting beige solid was washed with cold pentane and dried in vacuo at 60 °C. Yield: 273 mg (0.152 mmol, 55%). IR (C_6D_6): 1542 ($\nu_{\text{N-NH}}$). ^{1}H NMR (C_6D_6, 20 °C) δ: 8.43 (s, 1H, *J*(^{183}W-H) = 17.4 Hz, N=N*H*), 7.30 (br d, 6H, 4′,6′-*H*), 7.20 (s, 12H, 3,5,3″,5″-*H*), 6.64 (br t, 3H, 2′-*H*), 3.68 (br t, 6H, NCH_2), 3.14 (sept, J_{HH} = 6.6 Hz, 12H, 2,6,2″,6″-C*H*Me$_2$), 2.93 (sept, J_{HH} = 6.9 Hz, 6H, 4,4″-C*H*Me$_2$), 1.88 (br t, 6H, NCH_2), 1.37 (d, J_{HH} = 6.6 Hz, 36H, 4,4″-CH(CH_3)$_2$), 1.24 (d, J_{HH} = 6.6 Hz, 36H, 2,6,2″,6″-CH(CH_3)$_2$), 1.14 (d, J_{HH} = 6.6 Hz, 36H, 2,6,2″,6″-CH(CH_3)$_2$). Anal. calcd. for $C_{114}H_{160}N_6W$ (%): C 76.14, H 8.97, N 4.67; found: C 76.00, H 8.96, N 4.55.

X-ray quality crystals were obtained from a supersaturated heptane solution at room temperature.

[HIPTN$_3$N]W^{15}N=^{15}NH

W^{15}N=^{15}NK (40 mg) was treated with [Et$_3$NH][OTf] (1.05 equiv.) in C_6D_6 in an NMR tube to yield the title compound, 92% ^{15}N-enriched, essentially quantitatively. The solution was taken to dryness in vacuo and the residue was dissolved in C_6D_6 for spectroscopic analysis. IR (C_6D_6): 1499 ($\nu_{^{15}\text{N}-^{15}\text{NH}}$). ^{1}H NMR ($C_6D_6$, 20 °C) δ: 8.42 (s, 0.08H, ^{14}N$_\alpha$=^{14}N$_\beta$*H*), 8.41 (dd, ^{1}*J*(^{15}N$_\beta$-H) = 53.1 Hz, ^{2}*J*(^{15}N$_\alpha$-H) = 6.7 Hz, *J*(^{183}W-H) = 17.1 Hz, 0.92H, ^{15}N$_\alpha$=^{15}N$_\beta$*H*) (other resonances are identical to those measured for the unlabeled sample). ^{15}N NMR (C_6D_6, 20 °C) δ: 393.5 (dd, *J*(^{15}N$_\alpha$-^{15}N$_\beta$) = 15.8 Hz, ^{2}*J*(^{15}N$_\alpha$-H) = 6.5 Hz, ^{15}*N*$_\alpha$=^{15}N$_\beta$H), 229.3 (dd, ^{1}*J*(^{15}N$_\beta$-H) = 53.9 Hz, *J*(^{15}N$_\alpha$-^{15}N$_\beta$) = 14.9 Hz, ^{15}N$_\alpha$=^{15}*N*$_\beta$H).

{[HIPTN$_3$N]W=NNH$_2$}[BAr′$_4$]

An ether (4 mL) solution of **W**N=NH (100 mg, 55.6 μmol) was stirred and treated with solid [H(OEt$_2$)$_2$][BAr′$_4$] (59.1 mg, 58.4 μmol) at –35 °C. The solution was stirred for 1 h while being allowed to warm up to room temperature, and then taken to dryness in vacuo. The resulting solid was extracted with pentane and the pentane extracts were filtered through Celite® and concentrated to ~3 mL. Seeding this solution with a minute amount of {[HIPTN$_3$N]Mo=NNH$_2$}[BAr′$_4$] (33) led to a gradual formation of pale yellow microcrystals over a period of ~1 h. The mixture stood at –35 °C for several days and the product was isolated by filtration, washed with cold pentane, and dried in vacuo at 60 °C. Yield: 106 mg (39.8 μmol, 72%). ^{1}H NMR (C_6D_6, 20 °C) δ: 8.36 (br s, 8H, C$_6$H$_3$-3,5-(CF$_3$)$_2$-2,6-*H*), 7.66 (br s, 4H, C$_6$*H*$_3$-3,5-(CF$_3$)$_2$-4-*H*), 7.13 (s, 12H, 3,5,3″,5″-*H*), 6.79 (br d, 6H, 4′,6′-*H*), 6.62 (br t, 3H, 2′-*H*), 5.96 (s, 2H, *J*(^{183}W-H) ~ 6 Hz, N-NH_2), 3.78 (br t, 6H, NCH_2), 2.88 (sept, J_{HH} = 6.9 Hz, 6H, 4,4″-C*H*Me$_2$), 2.67 (sept, J_{HH} = 6.8 Hz, 12H, 2,6,2″,6″-C*H*Me$_2$), 2.32 (br t, 6H, NCH_2), 1.33 (d, J_{HH} = 6.6 Hz, 36H, 4,4″-CH(CH_3)$_2$), 1.11 (d, J_{HH} = 6.8 Hz, 36H, 2,6,2″,6″-CH(CH_3)$_2$), 0.98 (d, J_{HH} = 6.8 Hz, 36H, 2,6,2″,6″-CH(CH_3)$_2$). ^{19}F NMR (C_6D_6, 20 °C) δ: –62.4 (s, CF$_3$). Anal. calcd. for $C_{146}H_{173}BF_{24}N_6W$ (%): C 65.86, H 6.55, N 3.16; found: C 65.74, H 6.46, N 3.08.

X-ray quality crystals were obtained from a supersaturated heptane solution at room temperature.

{[HIPTN$_3$N]W=^{15}N^{15}NH$_2$}[BAr′$_4$]

W^{15}N=^{15}NH, generated in situ as described above, was treated with 1 equiv. of [H(OEt$_2$)$_2$][BAr′$_4$] in C_6D_6 in an NMR tube to yield the title compound, 92% ^{15}N-enriched, essentially quantitatively. ^{1}H NMR (C_6D_6, 20 °C) δ: 5.99 (s, 0.08 H, ^{14}N$_\alpha$-^{14}N$_\beta$$H_2$), 5.99 (dd, ^{1}*J*(^{15}N$_\beta$-H) = 83.6 Hz, ^{2}*J*(^{15}N$_\alpha$-H) = 1.8 Hz, 0.92 H, ^{15}N$_\alpha$-^{15}N$_\beta$$H_2$) (other resonances are identical to those measured for the unlabeled sample). ^{15}N NMR (C_6D_6, 20 °C) δ: 343.8 (d, *J*(^{15}N$_\alpha$-^{15}N$_\beta$) = 10.2 Hz, 1N, ^{15}*N*$_\alpha$-^{15}N$_\beta$H$_2$), 131.1 (td, ^{1}*J*(^{15}N$_\beta$-H) = 83.8 Hz, *J*(^{15}N$_\alpha$-^{15}N$_\beta$) = 9.9 Hz, 1N, ^{15}N$_\alpha$-^{15}*N*$_\beta$H$_2$).

[HIPTN$_3$N]W≡N

A mixture of **W**Cl (500 mg, 0.277 mmol) and NaN$_3$ (54.0 mg, 0.831 mmol) in a mixture of benzene and acetonitrile (4:6 mL) was stirred vigorously for 16 h. The mixture became lighter in color and was taken to dryness in vacuo. The solid residue was dried at 80 °C in vacuo and extracted with benzene. The benzene extracts were filtered through Celite® and the filtrates were taken to dryness in vacuo. Addition of pentane (3 mL) led to the precipitation of a pale beige solid after 1 h at room temperature. The mixture was allowed to stand at –35 °C for several days, and the product was then isolated by filtration, washed with cold pentane, and dried at 70 °C in vacuo. Yield: 286 mg (0.160 mmol, 58%). IR (C_6D_6): 1024 (ν_{Mo-N}). ^1H NMR (C_6D_6, 20 °C) δ: 8.01 (br s, 6H, 4′,6′-*H*), 7.21 (s, 12H, 3,5,3″,5″-*H*), 6.59 (s, 3H, 2′-*H*), 3.66 (br t, 6H, NCH_2), 3.10 (sept, J_{HH} = 6.6 Hz, 12H, 2,6,2″,6″-C*H*Me$_2$), 2.93 (sept, J_{HH} = 6.8 Hz, 6H, 4,4″-C*H*Me$_2$), 1.66 (br t, 6H, NCH_2), 1.37 (d, J_{HH} = 6.9 Hz, 36H, 4,4″-CH(CH_3)$_2$), 1.24 (d, J_{HH} = 6.6 Hz, 36H, 2,6,2″,6″-CH(CH_3)$_2$), 1.10 (br d, J_{HH} = 6.3 Hz, 36H, 2,6,2″,6″-CH(CH_3)$_2$). Anal. calcd. for $C_{114}H_{159}N_5W$ (%): C 76.78, H 8.99, N 3.93; found: C 76.57, H 9.01, N 3.94.

[HIPTN$_3$N]W≡^{15}N

[**W**=^{15}N^{15}NH$_2$][BAr′$_4$], generated in situ as described above, was treated with 2 equiv. of $CoCp^*_2$ in C_6D_6 in an NMR tube to yield a mixture consisting predominantly of **W**^{15}N=^{15}NH and the title compound. ^{15}N NMR (C_6D_6, 20 °C) δ: 827.0 (s, W≡^{15}*N*), 393.5 (dd, W^{15}N_α=^{15}N_βH), 229.3 (dd, W^{15}N_α=^{15}N_βH).

{[HIPTN$_3$N]W(NH$_3$)}[BAr′$_4$]

Ammonia (57 mL, 360 torr (1 torr = 133.322 Pa), ~1.11 mmol) was vacuum transferred from a bronze-colored Na solution to a frozen mixture of **W**Cl (500 mg, 0.277 mmol) and NaBAr′$_4$ (540.2 mg, 0.610 mmol) in fluorobenzene (10 mL). The mixture was thawed and stirred at room temperature for 2 h, at which time ^1H NMR analysis of an aliquot taken from the reaction mixture showed complete consumption of **W**Cl. The mixture was taken to dryness in vacuo, and the solid residue was dried at 60 °C and extracted with pentane. The pentane extracts were filtered through Celite® and the filtrate was concentrated to 3 mL. This solution was seeded with a minute quantity of crystalline {[HIPTN$_3$N]Mo(NH$_3$)}[BAr′$_4$], which led to rapid formation of a bright yellow microcrystalline solid. The mixture was left standing at –35 °C for several days and the product was then isolated by filtration, washed with cold pentane, and dried in vacuo at 60 °C, turning light orange. Yield: 642 mg (242 mmol, 87%). ^1H NMR (C_6D_6, 20 °C) δ: 18.66 (s, 6H, 8.27, 4′,6′-*H*), 7.41 (s, 12H, 3,5,3″,5″-*H*), 7.34 (s, 8H, C$_6$$H_3$-3,5-(CF$_3$)$_2$-2,6-*H*), 7.21 (s, 4H, C$_6$$H_3$-3,5-(CF$_3$)$_2$-4-*H*), 3.15 (sept, J_{HH} = 6.9 Hz, 6H, 4,4″-C*H*Me$_2$), 2.7 (v br s, 12H, 2,6,2″,6″-C*H*Me$_2$), 1.54 (d, J_{HH} = 6.6 Hz, 36H, 4,4″-CH(CH_3)$_2$), 1.01 (br s, 36H, 2,6,2″,6″-CH(CH_3)$_2$), 0.6 (v br s, 36H, 2,6,2″,6″-CH(CH_3)$_2$), –0.20 (s, 3H, 2′-*H*), –28.79 (s, 6H, NCH_2), –63.7 (br s, 6H, NCH_2). Anal. calcd. $C_{146}H_{174}BF_{24}N_5W$ (%): C 66.16, H 6.62, N 2.64; found: C 65.97, H 6.68, N 2.52.

X-ray quality crystals were obtained from a supersaturated heptane solution at room temperature.

[HIPTN$_3$N]WH$_3$

A benzene (5 mL) solution of [**W**(NH$_3$)][BAr′$_4$] (700 mg, 0.264 mmol) was treated with LiBHEt$_3$ (1 mol/L THF, 264 μL, 0.264 mmol) at room temperature. The resulting brown-red mixture was stirred for 30 min, freeze–pump–thaw degassed, and exposed to 1 atm of H_2 (1 atm = 101.325 kPa), which caused some lightening in color. The mixture was stirred for 1 h and brought to dryness in vacuo. The resulting solid was dried at 80 °C and extracted with benzene. The benzene extracts were filtered through Celite® and the filtrate was taken to dryness. Addition of pentane (4 mL) to the residue led to a gradual formation of a light brown solid. The mixture was left standing at –35 °C for several days and the product was then isolated by filtration, washed with cold pentane, and dried in vacuo at 70 °C. As was explained in the text, **W**H$_3$ loses hydrogen in the solid state at elevated temperatures under vacuum, forming an observable quantity of a paramagnetic compound tentatively assigned as the monohydride **W**H. Thus, solid **W**H$_3$ isolated as described previously was stored under an atmosphere of H_2 overnight, which nearly eliminated the **W**H impurity. Yield: 208 mg (0.117 mmol, 44%). IR (C_6D_6): 1966, 1958 (both broad, ν_{W-H}). ^1H NMR (C_6D_6, 20 °C) δ: 11.99 (s, 3H, J(^{183}W-H) = 24 Hz, W(*H*)$_3$), 7.66 (s, 6H, 4′,6′-*H*), 7.21 (s, 12H, 3,5,3″,5″-*H*), 6.54 (s, 3H, 2′-*H*), 3.65 (s, 6H, NCH_2), 3.10 (sept, J_{HH} = 6.8 Hz, 12H, 2,6,2″,6″-C*H*Me$_2$), 2.93 (sept, J_{HH} = 6.9 Hz, 6H, 4,4″-C*H*Me$_2$), 2.01 (s, 6H, NCH_2), 1.37 (d, J_{HH} = 6.9 Hz, 36H, 4,4″-CH(CH_3)$_2$), 1.24 (d, J_{HH} = 6.9 Hz, 36H, 2,6,2″,6″-CH(CH_3)$_2$), 1.12 (d, J_{HH} = 6.6 Hz, 36H, 2,6,2″,6″-CH(CH_3)$_2$). Anal. calcd. for $C_{114}H_{162}N_4W$ (%): C 77.25, H 9.21, N 3.16; found: C 77.08, H 9.28, N 3.06.

Acknowledgements

R.R.S. is grateful to the National Institutes of Health (GM 31978) for research support and both R.R.S. and D.V.Y. are grateful to William E. Geiger for advice on electrochemistry in weakly polar media.

References

1. A.D. Allen and C.V. Senoff. J. Chem. Soc. Chem. Commun. 621 (1965).
2. B.K. Burgess and D.J. Lowe. Chem. Rev. **96**, 2983 (1996).
3. B.K. Burgess. ACS Symp. Ser. **535**, 144 (1993).
4. B.K. Burgess. Chem. Rev. **90**, 1377 (1990).
5. J. Chatt, J.R. Dilworth, and R.L. Richards. Chem. Rev. **78**, 589 (1978).
6. M. Hidai and Y. Mizobe. Chem. Rev. **95**, 1115 (1995).
7. M. Hidai. Coord. Chem. Rev. **185–186**, 99 (1999).
8. M.D. Fryzuk and S.A. Johnson. Coord. Chem. Rev. **200–202**, 379 (2000).
9. T.A. Bazhenova and A.E. Shilov. Coord. Chem. Rev. **144**, 69 (1995).
10. C.J. Pickett. J. Biol. Inorg. Chem. **1**, 601 (1996).
11. F. Barriere. Coord. Chem. Rev. **236**, 71 (2003).
12. R.L. Richards. Coord. Chem. Rev. **154**, 83 (1996).
13. R.A. Henderson, G.J. Leigh, and C.J. Pickett. Adv. Inorg. Chem. Radiochem. **27**, 197 (1983).
14. J. Chatt and G.J. Leigh. Chem. Soc. Rev. **1**, 121 (1972).
15. A.D. Allen, R.O. Harris, B.R. Loescher, J.R. Stevens, and R.N. Whiteley. Chem. Rev. **73**, 11 (1973).
16. B.A. MacKay and M.D. Fryzuk. Chem. Rev. **104**, 385 (2004).
17. K. Komori, H. Oshita, Y. Mizobe, and M. Hidai. J. Am. Chem. Soc. **111**, 1939 (1989).

18. M. Mori, K. Hori, M. Akashi, M. Hori, Y. Sato, and M. Nishida. Angew. Chem. Int. Ed. **37**, 636 (1998).
19. K. Hori and M. Mori. J. Am. Chem. Soc. **120**, 7651 (1998).
20. M. Mori, M. Hori, and Y. Sato. J. Org. Chem. **63**, 4832 (1998).
21. M. Akashi and M. Mori. Heterocycles, **59**, 661 (2003).
22. K. Ueda and M. Mori. Tetrahedron Lett. **45**, 2907 (2004).
23. M. Mori. J. Heterocycl. Chem. **37**, 623 (2000).
24. M. Akashi, Y. Sato, and M. Mori. J. Org. Chem. **66**, 7873 (2001).
25. M. Akashi, M. Nishida, and M. Mori. Chem. Lett. 465 (1999).
26. M. Mori. J. Organometal. Chem. **689**, 4210 (2004).
27. A.E. Shilov. J. Mol. Catal. **41**, 221 (1987).
28. A.E. Shilov. Russ. Chem. Bull. Int. Ed. **52**, 2555 (2003).
29. R.R. Schrock. Pure Appl. Chem. **69**, 2197 (1997).
30. G.E. Greco and R.R. Schrock. Inorg. Chem. **40**, 3850 (2001).
31. G.E. Greco and R.R. Schrock. Inorg. Chem. **40**, 3860 (2001).
32. D.V. Yandulov and R.R. Schrock. J. Am. Chem. Soc. **124**, 6252 (2002).
33. D.V. Yandulov, R.R. Schrock, A.L. Rheingold, C. Ceccarelli, and W.M. Davis. Inorg. Chem. **42**, 796 (2003).
34. D. Yandulov and R.R. Schrock. Inorg. Chem. **44**, 1103 (2005).
35. D.V. Yandulov and R.R. Schrock. Science, **301**, 76 (2003).
36. G.M. Sheldrick. SADABS: A program for absorption correction of crystallographic data. Version 2.10 [computer program]. University of Goettingen, Goettingen, Germany. 1996.
37. V. Ritleng, D.V. Yandulov, W.W. Weare, R.R. Schrock, A.R. Hock, and W.M. Davis. J. Am. Chem. Soc. **126**, 6150 (2004).
38. S. Siemann, K. Schneider, M. Oley, and A. Mueller. Biochemistry, **42**, 3846 (2003).
39. G.E. Greco, A.I. Popa, and R.R. Schrock. Organometallics, **17**, 5591 (1998).
40. S.W. Seidel, R.R. Schrock, and W.M. Davis. Organometallics, **17**, 1058 (1998).
41. R.R. Schrock, S.W. Seidel, N.C. Mösch-Zanetti, K.-Y. Shih, M.B. O'Donoghue, W.M. Davis, and W.M. Reiff. J. Am. Chem. Soc. **119**, 11 876 (1997).
42. N.C. Mösch-Zanetti, R.R. Schrock, W.M. Davis, K. Wanninger, S.W. Seidel, and M.B. O'Donoghue. J. Am. Chem. Soc. **119**, 11 037 (1997).
43. R.R. Schrock, K.-Y. Shih, D. Dobbs, and W.M. Davis. J. Am. Chem. Soc. **117**, 6609 (1995).
44. M.G. Fickes, A.L. Odom, and C.C. Cummins. Chem. Commun. 1993 (1997).
45. J.C. Peters, A.L. Odom, and C.C. Cummins. Chem. Commun. 1995 (1997).
46. J.B. Greco, J.C. Peters, T.A. Baker, W.M. Davis, C.C. Cummins, and G. Wu. J. Am. Chem. Soc. **123**, 5003 (2001).
47. J.S. Figueroa and C.C. Cummins. Angew. Chem. Int. Ed. **43**, 984 (2004).
48. J. Mason. Chem. Rev. **81**, 205 (1981).
49. J. Mason. *In* Multinuclear NMR. *Edited by* J. Mason. Plenum Press, New York. 1987.
50. M.G. Hill, W.M. Lamanna, and K.R. Mann. Inorg. Chem. **30**, 4687 (1991).
51. N.G. Connelly and W.E. Geiger. Chem. Rev. **96**, 877 (1996).
52. R.J. LeSuer and W.E. Geiger. Angew. Chem. Int. Ed. **39**, 248 (2000).
53. N. Camire, U.T. Mueller-Westerhoff, and W.E. Geiger. J. Organomet. Chem. **637**–**639**, 823 (2001).
54. N. Camire, A. Nafady, and W.E. Geiger. J. Am. Chem. Soc. **124**, 7260 (2002).
55. S. Trupia, A. Nafady, and W.E. Geiger. Inorg. Chem. **42**, 5480 (2003).
56. M.B. O'Donoghue, W.M. Davis, and R.R. Schrock. Inorg. Chem. **37**, 5149 (1998).
57. D.A. Dobbs, R.R. Schrock, and W.M. Davis. Inorg. Chim. Acta, **263**, 171 (1997).
58. A.B. Pangborn, M.A. Giardello, R.H. Grubbs, R.K. Rosen, and F.J. Timmers. Organometallics, **15**, 1518 (1996).
59. C. Persson and C. Andersson. Inorg. Chim. Acta, **203**, 235 (1993).
60. M. Brookhart, B. Grant, and A.F. Volpe, Jr. Organometallics, **11**, 3920 (1992).
61. M. Witanowski, L. Stefaniak, S. Szymanski, and H. Januszewski. J. Magn. Reson. **28**, 217 (1977).
62. A.L. Chaney and E.P. Marbach. Clinical Chem. **8**, 130 (1962).
63. M.W. Weatherburn. Anal. Chem. **39**, 971 (1967).
64. T.T. Ngo, A.P.H. Phan, C.F. Yam, and H.M. Lenhoff. Anal. Chem. **54** (1982).
65. M.J. Dilworth and K. Fisher. Anal. Biochem. **256**, 242 (1998).

This article has been cited by:

1. Jeremy M. Smith, Deepak Subedi. 2012. The structure and reactivity of iron nitride complexes. *Dalton Transactions* **41**:5, 1423. [CrossRef]
2. Richard R. SchrockCatalytic Reduction of Dinitrogen to Ammonia by Molybdenum 25-50. [CrossRef]
3. Michael R. Reithofer, Richard R. Schrock, Peter Mu#ller. 2010. Synthesis of [(DPPNCH 2 CH 2) 3 N] 3- Molybdenum Complexes (DPP = 3,5-(2,5-Diisopropylpyrrolyl) 2 C 6 H 3) and Studies Relevant to Catalytic Reduction of Dinitrogen. *Journal of the American Chemical Society* **132**:24, 8349-8358. [CrossRef]
4. Richard R. Schrock. 2008. Catalytic Reduction of Dinitrogen to Ammonia by Molybdenum: Theory versus Experiment. *Angewandte Chemie International Edition* **47**:30, 5512-5522. [CrossRef]
5. Richard R. Schrock. 2008. Die katalytische Reduktion von Distickstoff zu Ammoniak mit Molybdän: Theorie und Experiment. *Angewandte Chemie* **120**:30, 5594-5605. [CrossRef]
6. Christopher J. PickettMolecular Nitrogen and Dinitrogen Complexes . [CrossRef]
7. Markus Hölscher, Walter Leitner. 2006. DFT Investigation of the Potential of [H-M{(NHCH2CH2)3X}] Catalysts (M = Mo, Ru, Os; X = N, P) for the Reduction of N2 to NH3 by H2. *European Journal of Inorganic Chemistry* **2006**:21, 4407-4417. [CrossRef]
8. Alastair J. Nielson, Chaohong Shen, Joyce M. Waters. 2006. Molecular engineering of coordination pockets in chloro-tris-phenoxo complexes of titanium(IV). *Polyhedron* **25**:10, 2039-2054. [CrossRef]